

**Broadband dielectric spectroscopy of Nafion-117, sulfonated polysulfone (sPSF) and sulfonated polyether ketone (sPEK) membranes**

**Wasim F. G. Saleha<sup>1,2</sup>, Rahul Ramesh<sup>2</sup>, Nalajala Naresh<sup>1,2</sup>, Arup Chakraborty<sup>2</sup>, Bradley P. Ladewig<sup>3</sup> and Manoj Neergat<sup>2,\*</sup>**

<sup>1</sup>IITB-Monash Research Academy, Powai, Mumbai, India-400076

<sup>2</sup>Department of Energy Science and Engineering, Indian Institute of Technology Bombay (IITB), Mumbai, India-400076

<sup>3</sup>Department of Chemical Engineering, Imperial College London, Exhibition Road, London SW7 2AZ, United Kingdom

**ABSTRACT**

Nafion<sup>®</sup>-117, sulfonated polysulfone (sPSF) and sulfonated polyetherketone (sPEK) are characterized using broadband dielectric spectroscopy in the frequency range of 10 MHz–100 mHz. Overall, there are 4-5 relaxation processes in these sulfonated membranes and a comparison of their spectral features allows assigning the relaxation processes. At an optimum amplitude of  $\sim 100$  mV<sub>rms</sub>, all the relaxations are clearly defined as the electrode polarization is minimized. At low temperatures ( $-130^{\circ}\text{C}$ ), these membranes show a broad relaxation peak in the mid-frequency region, which quickly shifts towards the high-frequency region as the temperature is increased to  $-90^{\circ}\text{C}$ . This peak is observed in proton exchange membranes for the first time due to the use of low ac amplitude, and it is assigned to the relaxation of the confined water in the micro-pores. With all the membranes, the peak associated with  $-\text{SO}_3\text{H}$  group relaxation is observed in the same frequency range at a temperature of  $\sim -80^{\circ}\text{C}$ .

\*Corresponding author. Tel.: +91 22 2576 7893; Fax: +91 22 2576 4890

E-mail address: [nmanoj@iitb.ac.in](mailto:nmanoj@iitb.ac.in)

## INTRODUCTION

Broadband dielectric spectroscopy (BDS) is extensively used to investigate a wide range of inorganic, organic, and polymeric materials.<sup>1-3</sup> These investigations include molecular dynamics and conductivity in polymers of intrinsic microporosity (PIM), proton transport in multi-scale hybrid membranes and supramolecular hydrogen bonded-network.<sup>4-7</sup> Moreover, BDS is used to investigate composite membranes, the effect of casting solvent and concentration on polymer blends, and to track kinetics of step growth polymerization process.<sup>8-11</sup> Thus, Tarnacka *et al.* concluded that polymerization under confinement is much faster than that in bulk.<sup>11</sup> Recently, Di Noto *et al.* and Sood *et al.* investigated electrical properties of Nafion neutralized and doped with proton conducting ionic liquids.<sup>12,13</sup> Zaneta *et al.* reviewed the progress in dielectric properties of protic ionic liquids (PIL).<sup>14</sup>

Proton conducting polymer electrolyte membranes are an important class of materials used in a wide range of electrochemical energy conversion and storage devices (fuel cells, electrolyzers, and flow batteries). In general, these membranes are constituted with aliphatic or aromatic polymer backbone, side-chains and functional groups. The polymer backbone imparts mechanical strength and structural integrity. Side-chains and substituted functional groups facilitate the proton conduction. The high proton conductivity, mechanical properties and chemical stability of the polymer originate from its unique structure (**Figure 1a**).<sup>15</sup> This type of polymer electrolyte membranes have water-assisted conduction mechanism and therefore their operating temperature is limited to ~150°C under pressurized conditions.<sup>15,16</sup> Devices employing these membranes undergo several start/stop cycles involving drying/rehydration and cold start-up from extremely low temperatures (~-50°C). On the other hand, under hot conditions, the temperature can exceed ~100°C and it results in the decreased water content and hence reduced

conductivity of the membrane.<sup>17-19</sup> Thus, the membranes are subjected to a broad range of temperature. Therefore, understanding the dynamics of polymer electrolyte membranes (PEMs) with temperature is paramount.

Among PEMs, Nafion is the state of the art membrane. Nafion is highly expensive and efforts are made to replace it with cheaper alternatives; sulfonated polysulfone (sPSF) and polyaryletherketones (sPEEK and sPEK) are two of the promising candidates (Figures 1b, c and d).<sup>20-28</sup> In general, as mentioned earlier, these membranes have three common attributes. The polymeric main-chain (aliphatic/aromatic), side-chain/main-chain substituted functional groups, and water-assisted proton conduction mechanism. Water of hydration facilitates the transport of  $H^+$  ions through the membranes and it is highly dependent on the degree of sulfonation and the operating temperature.<sup>29-33</sup> All the three membranes have the same functional group ( $SO_3H$ ), but their degree of sulfonation is different. Only Nafion has the side-chain and sPSF and sPEK lack the same.

Among these membranes, Nafion has been investigated using BDS.<sup>32-45</sup> On the other hand, the other two sulfonated polymers (sPSF and sPEK) are seldom investigated. Various relaxations originating from the backbone, functional group and side-chain are reported in the literature. The assignment of the relaxations to various physical processes is not conclusive, and there is no consensus on the relaxation processes. For instance, Hassan *et al.* attributed  $\alpha$  and  $\beta$  relaxations to the segmental motion;  $\alpha$  relaxation to the polymer backbone fluctuations (glass-transition processes), while  $\beta$  relaxation to the fluctuations of  $-SO_3H$  group or the side-chain attached to the fluorocarbon main-chain.<sup>41</sup> However, Matos *et al.* assigned the  $\alpha$  and  $\beta$  relaxation to the counter ion motion of the rod-like polymer aggregate along the longitudinal and radial directions, respectively.<sup>44,45</sup> Other than these processes due to the motion of the dipoles in the polymer, in

some reports, the  $\beta$  relaxation is assigned to the interfacial and electrode polarization.<sup>46–48</sup> Similarly, the PSF membrane shows three major relaxations in which the  $\alpha$  relaxation is associated with the glass-transition process observed at  $\sim 185^\circ\text{C}$ .<sup>49,50</sup> The relaxation observed at  $\sim 80^\circ\text{C}$  is assigned to backbone fluctuation, which is also termed as packing defect relaxation and the third relaxation observed at a very low temperature of  $-100^\circ\text{C}$  is a subject of debate. Its origin is generally assigned to phenyl ring fluctuation or movement of sulfone side group. Moreover, the relaxation originating from water is not reported with proton conducting membranes.

Therefore, BDS spectra of Nafion, sPSF, and sPEK membranes are recorded and analyzed over a broad range of temperature and frequency. Based on the activation energy, frequency range and the movement of the relaxation peak with temperature, we could convincingly assign the relaxation processes by comparison and elimination. For e.g., the relaxation of  $\text{SO}_3\text{H}$  groups at a given temperature appears at a particular frequency with all the membranes. The side-chain relaxation was confirmed by its absence in sPSF. The water relaxation is common in all the three membranes at the same temperature and frequency ranges.

< **Figure 1** >

## **EXPERIMENTAL**

### **Materials / Chemicals**

Nafion<sup>®</sup>-117 and polysulfone (MW: 35,000) from Sigma Aldrich; polyether ketone (PEK) powder (grade 1300P) from Gharda Chemicals; *p*-chlorophenol from Loba Chemie; sulfuric acid (98%), peroxide solution ( $\text{H}_2\text{O}_2$ , 30%), hydrochloric acid (HCl), chlorosulfonic acid, N,N-

dimethyl-formamide, sodium hydroxide (NaOH), and 1, 2-dichloroethane (DCE) from Merck were used without further treatment. De-ionized (DI) water was obtained from Direct-Q Millipore de-ionizer.

### ***Treatment of Nafion-117 membrane***

A piece of commercial Nafion-117 membrane (10 cm x 10 cm) was boiled for 30 min each in 3% H<sub>2</sub>O<sub>2</sub> solution, DI water, and 2 M HCl. Thereafter, it was boiled in DI water for 30 min to remove traces of surface acid.<sup>51</sup>

### **Sulfonation of Polysulfone**

Required amount of PSF (4.8 g) was dissolved in 50 mL of 1, 2-dichloroethane (DCE) by mechanical stirring at 60°C for 2 h.<sup>52</sup> Then, a solution of 0.6 mL chlorosulfonic acid in 10 mL of DCE was prepared separately in a 100 mL beaker and it was added drop-wise to the polymer solution kept at 60°C under nitrogen purging; this process yields the desired membrane property (ion exchange capacity of ~1.2 meq g<sup>-1</sup> and ~60% degree of sulfonation). The reaction product was neutralized in DI water several times and the transparent jelly-type sulfonated polymer was filtered and dried overnight at 80°C.

### ***Preparation of sPSF membrane***

The desired amount of the sulfonated polymer (200 mg), prepared as mentioned above, was dissolved in 10 mL of N-N-dimethyl-formamide at room temperature for 2 h. The solution was poured on a glass substrate to form a uniform layer and it was dried in a vacuum oven for 24 h at 60°C. The dried membrane (40 µm thick) was washed repeatedly with DI water to remove any surface impurities.

### **Sulfonation of Polyetherketone (PEK)**

The required amount of fine PEK powder (15 g) was slowly added to 55 mL of concentrated H<sub>2</sub>SO<sub>4</sub> taken in a 250 mL beaker. The mixture was stirred with a glass rod to get homogenous polymer dispersion. It was stirred again for 24 h at room temperature to ensure complete sulfonation of PEK.

### ***Preparation of sPEK membrane***

To prepare the sPEK membrane by the phase-inversion method, the deep red sulfonated polymer solution (prepared as mentioned above) was uniformly spread on a glass plate using a doctor blade. It was then immersed in DI water to obtain the sPEK membrane film. The thickness (150 μm) of the membrane was controlled by choosing appropriate quantity of the solution, exposure time, and casting area.

### **Differential scanning calorimetry (DSC)**

The glass transition temperature ( $T_g$ ) of the polymers was determined with differential scanning calorimetry (DSC Q20, TA instruments). All DSC runs were carried out in the temperature range of 25–240°C at a heating rate of 10°C min<sup>-1</sup> under nitrogen atmosphere to minimize the oxidative degradation; the second heating cycle was used to calculate the  $T_g$ . Before all DSC experiments, the baseline was calibrated using empty aluminum pans and a sample of ~4 mg was used in each case.

### **Broadband dielectric spectroscopy (BDS)**

The dielectric properties of PEMs were investigated using Novocontrol Concept 80, NOVOCONTROL Technologies, Germany. The membrane was sandwiched between two platinum electrodes of one cm diameter and was analyzed in the frequency range of 10 MHz–0.1 Hz at a temperature range of -130 – 220°C; the dielectric response was measured with an ac

amplitude of 100 mV rms during the heating cycle. The use of large amplitudes (for e.g., 1 V typically reported for conducting membranes) causes high polarization and it masks the feeble relaxations. All the membranes were subjected to similar conditioning prior to recording the BDS spectra. The relaxation peaks were fitted with Havriliak-Negami equation using the WinFit software.

## RESULTS AND DISCUSSION

### Ion exchange capacity (IEC) and degree of sulfonation (DS)

The degree of sulfonation determines the water retention properties and proton conductivity of sulfonated ionically conducting polymer materials. The IEC and DS (shown in the **Table 1**) were calculated following the titration method reported in the literature; the details are given in the supporting information (SI).<sup>21,53</sup> The water content in the membranes prior to the BDS characterization was found to be 18, 14 and 13% for Nafion-117, sPSF and sPEK, respectively, and it plays a major role in the polymer chain relaxations. The magnitude of dielectric loss ( $\epsilon''$ ) is directly proportional to the degree of sulfonation; more the sulfonated groups in the polymer chain, higher is the  $\epsilon''$  and the increase is also partly due to the electrode and interfacial polarization (see the discussion below).<sup>12</sup>

<**Table 1**> Ion exchange capacity and degree of sulfonation of the membranes

The morphology of a polymer and the chain relaxations are also a function of the casting technique and the degree of crystallinity of the polymer.<sup>54</sup> Nafion-117 has been cast using solvent evaporation method and also by extrusion technique; both the methods have profound impact on the chain orientation, crystallinity and hence the proton conductivity.<sup>55,56</sup> sPSF was

cast using a low boiling point solvent by evaporation at 60°C; this membrane has some degree of crystallinity due to slow drying.<sup>54</sup> To confirm the extent of crystallinity in sPEK, the XRD patterns of PEK powder, sPEK membrane cast from *p*-chlorophenol, and sPEK cast through phase-inversion method were recorded (**Figure S1**). The membrane cast using *p*-chlorophenol was dried on a hot-plate at a temperature of 80°C in a fumehood. The slow drying induces crystallinity and the XRD pattern of sPEK, with all the prominent peaks, almost matches with that of PEK powder. However, the XRD pattern of sPEK cast through phase-inversion method, using concentrated H<sub>2</sub>SO<sub>4</sub> as the solvent, shows a single broad peak. Thus, as observed from the XRD patterns(Figure S1), the porous PEK obtained by the phase-inversion method results in a highly amorphous polymer structure.<sup>57,58</sup>

### **Broadband dielectric spectroscopy (BDS)**

The relaxations are conventionally assigned as  $\delta$ ,  $\gamma$ ,  $\beta$  (secondary) and  $\alpha$  (primary) depending on the order they enter the frequency window with temperature. The low-temperature secondary relaxations are associated with the side-chain/rotational motions, and the small functional group motions. The  $\alpha$  relaxation (associated with the glass-transition) generally appears at higher temperature and it involves the motion of the amorphous polymer chain segments and the associated environment (co-operative motion).

**Figure 2** shows the 3D surface plot of  $\epsilon''$  as a function of frequency and temperature with Nafion-117, sPSF and sPEK membranes. The increase in dielectric loss of Nafion-117 membrane (Figure 2a) with temperature in the low-frequency (LF) region is mostly associated with the dc conductivity, electrode polarization, interfacial polarization and the activation of relaxation processes; at lower frequency and higher temperature, these effects significantly contribute to the total dielectric loss, while at higher frequency their effects are negligible.<sup>5,7,59</sup>



## < Figure 2 >

The dielectric data of Nafion-117 at various ac amplitudes are shown in the **Figure S2**. The effect of ac amplitude is clear from the low frequency region, and with the increase in amplitude there is a significant increase in the dielectric loss. Thus, with low ac amplitudes (100 mV<sub>rms</sub>) such aberrations can be avoided. The  $\epsilon''$  3D surface plots of sPSF and sPEK (Figures 2b and c) show similar trends in the dc conductivity at the LF region. In the case of sPSF membrane, the intensity of the  $\epsilon''$  rises with temperature upto  $\sim 80^\circ\text{C}$  until the water content is intact, but, it increases sharply with temperature beyond  $\sim 170^\circ\text{C}$ ; this may be attributed to the electrode polarization due to the presence of large number of free ions (high degree of sulfonation).<sup>6,59</sup> With sPEK there is a sudden drop in the intensity above  $\sim 100^\circ\text{C}$  and a sharp increase is observed at further higher temperature ( $>150^\circ\text{C}$ ). However, the extent of electrode polarization in sPEK is significantly lower (by several orders of magnitude of  $\epsilon''$  intensity), perhaps due to its low degree of sulfonation.

**Figure S3** shows the real conductivity of all the membranes derived from the BDS. In Figure S3a, Nafion-117 shows a conductivity of  $10^{-13}$  to  $10^{-3}$  S cm<sup>-1</sup> in the temperature range of  $-130 - 130^\circ\text{C}$ ; the conductivity rises with temperature upto  $80^\circ\text{C}$  and remains at  $\sim 10^{-3}$  S cm<sup>-1</sup> even at  $130^\circ\text{C}$ . Whereas with sPSF, the conductivity decreases due to the loss of water at temperature above  $70^\circ\text{C}$ . The unusual conductivity trend with Nafion may be due to the water evaporation and subsequent chain packing, which results in water-less proton hopping among the closely packed  $-\text{SO}_3\text{H}$  ions rather than through hydronium ions.<sup>41</sup> However, in the case of sPEK membranes, the highest conductivity observed is  $10^{-6}$  S cm<sup>-1</sup> and increment in conductivity with temperature is observed only upto  $\sim 40^\circ\text{C}$ ; above this temperature it decreases gradually. The low

degree of sulfonation and rapid loss of unbound water may be the reasons for the low conductivity and its decreasing trend.

From the 3D surface plots, only the major relaxations can be observed as ribs in the central part of the plot. Other relaxations not directly apparent in the 3D surface plots are marked after careful analysis of various plots (waterfall plot, Tan  $\delta$  vs. temperature (at  $\sim 1$  Hz), Tan  $\delta$  vs. frequency (at every  $10^\circ\text{C}$ ), and real permittivity ( $\epsilon'$ ) vs. frequency plots). The waterfall plots are included in the SI (**Figures S4, S5 and S6**). From, the Tan  $\delta$  vs. temperature plot at a given frequency (**Figure 3**), the presence of the different relaxations is apparent as separate peaks in the whole temperature range. The plot of dielectric loss vs. frequency is analyzed to mark the temperature range of a particular relaxation. All these plots are referred to identify the various relaxations.

< **Figure 3** >

Once the number of relaxations for a particular polymer system is thus identified at a given temperature, the  $\epsilon''$  is fitted using the Havriliak-Negami (HN) equation (Equation 1).

$$\epsilon^*(\omega) = \epsilon'(\omega) - i\epsilon''(\omega) = -i\left(\frac{\sigma_{dc}}{\epsilon_0(\omega)}\right)^N + \sum_{K=1}^3 \left[ \frac{\Delta\epsilon_k}{1 + \left((i\omega\tau_{HN})^{\alpha_k}\right)^{\beta_k}} + \epsilon_{\infty k} \right] \dots\dots\dots(1)$$

where,  $\epsilon'$ ,  $\epsilon''$  and  $\epsilon_0$  are the real, imaginary and vacuum permittivity, respectively,  $\omega$  ( $2\pi f$ ) is the frequency, and  $k$  is the number of relaxation terms which varies from 1 to 3. For each relaxation, dielectric strength ( $\Delta\epsilon_k = (\epsilon_R - \epsilon_\infty)_k$ ) is the difference between  $\epsilon'$  at very low and very high frequencies. In the first term,  $\sigma_{dc}$  is the dc conductivity and N characterizes conduction in terms

of the nature of charge hopping pathways – degree of morphological order and macromolecular dynamics.<sup>36,41</sup> Using this equation, all the useful parameters – relaxation time, dielectric strength, dc conductivity, and shape parameters – can be derived. In the following discussion, depending on the number of relaxations at a particular temperature, the  $\epsilon''$  is fitted with 1, 2 or 3 HN functions at every 10°C in the temperature range of -130 – 220°C. At temperature above ~170°C, the data could not be fitted due to the high intensity of the dielectric loss caused by the increase in dc conductivity and electrode polarization.

Based on the above discussion, to elucidate the deconvolution of the relaxation peaks, the  $\epsilon''$  of Nafion-117 (at -40°C and 10°C) is fitted with 3HN functions as shown in **Figure 4**;

< **Figure 4** >

With increase in temperature from -40°C (Figure 4a) to 10°C (Figure 4b), there is a significant rise in the dc conductivity and it dominates in the LF and MF regions. Inset to Figure 4b shows the magnified view of the fitted data at 10°C. The conductivity subtracted data clearly show a shoulder peak at the HF region ( $\delta$  relaxation) and a peak at the LF region ( $\beta$  relaxation). On the other hand, the experimental data show only one prominent peak at the HF region ( $\gamma$  relaxation). Thus, the DC conductivity features masks the relaxation peaks. All the deconvoluted relaxation peaks fitted at various temperatures are separately plotted to track the individual peak movement and the changes in the  $\Delta\epsilon$  of the relaxation process (**Figures S7** and **S8**). The deconvoluted peaks and their regular trend indicate the accuracy of fitting. With temperature, a given relaxation peak may shift toward the HF or LF region depending on the ease of the relaxation process and the morphological changes in the polymer.

The fitting results with sPSF at two different temperatures are shown in **Figure S9**. At a temperature of -20°C (Figure S9a), the data are fitted with 2HN functions corresponding to the  $\delta$

and  $\beta$  relaxations. As with Nafion-117, sPSF shows high dc conductivity at LF and MF regions and the relaxation peaks are barely discernible. The insets to the figure show distinctly visible deconvoluted peaks those further shift to HF region at 20°C (Figure S9b). **Figure S10** shows the fitted data of sPEK at a temperature of -90°C with 3HN functions corresponding to the  $\zeta$ ,  $\delta$ , and  $\gamma$  relaxations. With a negligible peak intensity and a complete shift to the HF region ( $\sim 10^7$  Hz), the  $\zeta$  relaxation is barely visible; but the  $\zeta$  peak at -90°C can be observed in Figure S7c.

### ***Relaxations in the temperature range of -130 – -90°C***

#### **(a) $\zeta$ relaxation**

The relaxation peak at the lowest temperature (-130°C) is feeble and it is difficult to resolve the same from the 3D surface plots or the  $\varepsilon''$  vs frequency plots (Figures 2 and 5). But, the presence of a relaxation can be clearly observed from the Tan  $\delta$  plot (Figure 3). This relaxation peak quickly shifts towards the HF region and it exists only for a short temperature range (-130 – -80°C). Di Noto *et al.* assigned a relaxation peak in the temperature range of -155 – -100°C to  $\gamma$  relaxation originating from the rotation of the -CF<sub>2</sub>- units in the PTFE backbone of Nafion; the peak appears at a frequency of 10 mHz at -155°C and shifts to 10<sup>7</sup> Hz by  $\sim$ -100°C.<sup>39</sup> But, the relaxation peak appearing at -130°C in the frequency range of 10–100 Hz is observed with all the three membranes ( $\sim$ 1000 Hz in case of sPEK) (Figure S7), including those without -CF<sub>2</sub>- backbone. The fast shift in peak position with increase in temperature indicates that the relaxation is due to those species whose movement is activated significantly with a minor change in temperature (Figures 5 and S7). With all the three membranes, the  $\Delta\varepsilon$  increases with temperature, but it is very low compared to that of the other relaxations. The peak distribution is very large (Figure S7) and its low intensity and broad nature suggest that the peak may be due to the relaxation of the confined water.<sup>60</sup> Similar observations at comparable frequency and

temperature ranges are reported in the literature for water in aqueous binary glass-formers, MCM-41 and other porous inorganic and organic materials.<sup>60–64</sup> The relaxation analysis carried out in the cooling cycle with Nafion-117 is shown in the **Figures S11** and **S12** and it is clear that the water relaxation peak is missing in the dry samples. This confirms that the feeble peak at lower temperatures is indeed due to water relaxations. In the BDS literature dealing exclusively with the water behavior, the relaxations were assigned as  $\alpha$  and  $\beta$  based on the phase of water.<sup>64</sup> In this report, the relaxations are marked based on the ease of the relaxation (smaller to larger molecules). Hence, the relaxation arising from the confined water in all the membranes is referred as  $\zeta$  relaxation.

#### < **Figure 5** >

Moreover, a paper by Cervený *et al.* which reviews the glass transition and relaxation in supercooled water, states that several polymeric systems (poly(methyl methacrylate), cellulose, polyimide-poly(dimethylsiloxane)s, poly(vinyl alcohol), and poly(aryl prehnitimide)) exhibit the presence of confined water.<sup>60</sup> All these systems, show the relaxation due to confined water at a temperature of  $\sim -133^\circ\text{C}$  and the average activation energy ( $E_A$ ) is found to be  $44 \text{ kJ mol}^{-1}$ . This is comparable to that obtained with the sulfonated membranes ( $38.10$ ,  $40.4$ , and  $41.35 \text{ kJ mol}^{-1}$  for Nafion-117, sPSF and sPEK, respectively) (discussed in the SI, **Figure S13** and **Table S1**). Therefore, based on the above discussion, the relaxation in the temperature range of  $-130 - -90^\circ\text{C}$  is attributed to the confined water in the polymer matrix.

At very low temperatures, water in the polymeric systems might be present in the form of both liquid water and crystallized ice; the pores which are smaller than  $\sim 20\text{\AA}$  or area near the walls (adjacent to molecules/functional groups) of the pores are reported to restrict crystallization.<sup>61,64</sup> The pore diameter in case of hydrated Nafion-117, sulfonated polyether ketones and

polysulfone-based sulfonated polymers is in the range of 1–2.5 nm.<sup>15,65,66</sup> Therefore, as the temperature increases from -130 – -90°C, the crystallized water changes to liquid phase and it causes increase in the intensity of the  $\epsilon''$ .

Apart from  $\zeta$  relaxation, Nafion-117 shows two more relaxations in this temperature range, whereas, sPSF and sPEK show one each. These relaxations are discussed in detail in the following sections.

### ***Relaxations in the temperature range of -100 – 20°C***

#### **(b) $\delta$ relaxation**

The second relaxation peak enters the frequency window at  $\sim$ -100°C even before the first peak ( $\zeta$  relaxation) vanishes out of the frequency range (Figure 5). This relaxation appears approximately in the same frequency range with all the membranes and shifts to higher frequency with temperature (Figure S8). In semi-fluorinated polysulfone (SF-PSF), the relaxation at comparable temperature range was assigned to the dipole fluctuations of SF side-chain.<sup>49</sup> However, even with the non-fluorinated sPSF and sPEK, a relaxation peak is observed in the same temperature range.

**Figures 6** and S8 show the trend of the second relaxation in all the three membranes in the temperature range of -80 – -20°C. With Nafion (Figure 4) the peak at  $\sim$ -100°C shifts fast to higher frequencies; at  $\sim$ -100°C, the peak maximum is at 1 Hz and by -50°C it moves to  $\sim$ 10<sup>4</sup> Hz (Figure S8). The frequency of the peak depends significantly on the water content in the membrane and hence the free volume in the polymer.<sup>37,39</sup> A peak in the same temperature and frequency range reported by Di Noto *et al.* was assigned to the fluctuation of -SO<sub>3</sub>H group and associated carbon in case of Nafion.<sup>39</sup> Here, this relaxation observed with all the three membranes (Nafion-117, sPSF and sPEK) is designated as  $\delta$ . In the temperature range of -80 – -20°C, a peak is observed in the LF range with sPSF; Tsuiji *et al.* investigated BDS of SF and -

COOH grafted polysulfone and assigned this peak to  $\gamma$  relaxation; it is observed at very low temperature ( $-100^{\circ}\text{C}$ ) at a frequency of 1 Hz, and  $E_A$  reported is  $46\pm 2 \text{ kJ mol}^{-1}$ .<sup>49</sup> The  $\gamma$  relaxation was assigned to the non-cooperative local fluctuation of the bisphenol group, or sulfone group in PSF backbone.<sup>49</sup> Some researchers assigned the  $\gamma$  relaxation to the rotation of phenyl ring.<sup>67-69</sup>

The attachment of -COOH group to the backbone slows down the  $\gamma$  relaxation process, which strengthens the theory that this relaxation is due to the movement of bisphenol group rather than the sulfone functional group. The hydrophilic nature of COOH-PSF results in higher hydrogen bonding and intermolecular interaction, which shift the relaxation to higher temperature.<sup>49</sup> With sPSF, at comparable temperature range, the relaxation peak shows an  $E_A$  of  $51.33 \text{ kJ mol}^{-1}$ . The relaxation may be attributed to the phenyl group motion, but the attachment of -SO<sub>3</sub>H group slows down the motion and therefore it occurs at slightly higher temperature and at lower frequency ( $\sim 1 \text{ Hz}$ ); the relaxation is observed at a temperature range of  $-100 - -20^{\circ}\text{C}$ , which is slightly higher when compared to the  $\gamma$  peak reported in the literature. Probably the -SO<sub>3</sub>H attachment onto one of the phenyl ring reduces the fluctuation associated with  $\gamma$  relaxation (slightly higher  $E_A$ ). Hence the observed  $\delta$  relaxation can be assigned to the fluctuation of -SO<sub>3</sub>H group with phenyl ring wagging motion or may be due to the movement of phenyl ring adjacent to the sulfonated phenyl ring.

In case of sPEK, in the temperature range of  $-100 - 0^{\circ}\text{C}$ , a second relaxation peak ( $\gamma$ ) is observed which spans through the entire frequency range (Figure 6). Leonardi *et al.* reported an  $E_A$  of  $56 \text{ kJ mol}^{-1}$  to a relaxation appearing in PEEK polymer; they attributed this relaxation to the phenyl ring rotation between the ether linkages.<sup>70</sup> In the similar temperature range, the peak observed with sPEK also shifts through the entire frequency range and has an  $E_A$  of  $44.62 \text{ kJ mol}^{-1}$  (Table S1). With PEEK, this relaxation was attributed to the phenylene ring rotation by Leonardi *et al.*

But in sPEK, with comparatively low  $E_A$ , it may be attributed to the  $-\text{SO}_3\text{H}$  relaxation along with the attached phenyl ring rotation.

< **Figure 6** >

The interesting characteristic of  $\delta$  relaxation is the unique trend in  $\Delta\epsilon$  depending on the degree of sulfonation, the polymer microstructure and the position of the  $-\text{SO}_3\text{H}$  group on the main-chain. With Nafion-117, the peak enters the frequency window from  $-110^\circ\text{C}$  and it moves towards HF region with increasing intensity ( $\Delta\epsilon$ ) upto  $20^\circ\text{C}$  (**Figure S14**). At further higher temperature, the intensity decreases significantly. This is a critical observation and can be helpful in understanding the underlying process that corresponds to the  $\delta$  relaxation. In the temperature range mentioned above ( $-20 - 90^\circ\text{C}$ ), water mostly exists in the liquid form, and therefore, a large number of polymer chains show the relaxation process. Freezing of water below  $-20^\circ\text{C}$  and its evaporation above  $90^\circ\text{C}$ , restricts the chain motions and results in lower  $\Delta\epsilon$ . Hence, the liquid water has a pronounced impact on the dielectric strength ( $\Delta\epsilon$ ) and the relaxation phenomenon. However, the  $\Delta\epsilon$  trend with sPSF is almost comparable to that of Nafion upto  $\sim 100^\circ\text{C}$ , but above this temperature, it sharply increases until  $180^\circ\text{C}$ . As expected, the relaxation peak shifts towards the lower frequencies. But the continuous increase in  $\Delta\epsilon$  even at higher temperatures suggest that the  $-\text{SO}_3\text{H}$  relaxation process becomes independent of water content and with higher thermal energy the complete chain motion happens. In case of sPEK, the  $\Delta\epsilon$  in this relaxation is  $\sim 3$  orders lower compared to that of the other two membranes in the same temperature range. The low  $\Delta\epsilon$  value can be attributed to the lower degree of sulfonation and subsequently the lesser number of species involved in the relaxation process. Due to the high fluctuation in the  $\epsilon''$  intensity above  $\sim 40^\circ\text{C}$  (3D surface plot, Figure 2), the sPEK data could be fitted only upto  $60^\circ\text{C}$ .



### (c) $\gamma$ relaxation

In Nafion-117, a third peak appears in quick succession following the  $\delta$  relaxation, unlike that with sPSF and sPEK; both the relaxations ( $\delta$  and  $\gamma$ ) enter the frequency window at  $\sim 90^\circ\text{C}$  and shift towards the higher frequency (Figure 6a). Since the  $-\text{SO}_3\text{H}$  functional group is attached to a side-chain, which is then connected to main-chain, Nafion can be considered as a Type C polymer (having flexible polar chain).<sup>1</sup> The long perfluorinated side-chain with a  $-\text{SO}_3\text{H}$  group at the end is highly flexible and that might be the origin of the two relaxations. One of the peaks is assigned to the  $-\text{SO}_3\text{H}$  motion (the  $\delta$  relaxation as discussed above) and second peak is indicated as  $\gamma$  relaxation. While in case of sPSF, the dipole (here the  $-\text{SO}_3\text{H}$  group) is directly attached to the main-chain and it is a Type B polymer (dipole rigidly attached to the main-chain).<sup>1</sup> The appearance of the  $-\text{SO}_3\text{H}$  motion is observed at the same temperature of  $\sim 100^\circ\text{C}$ , but only Nafion-117 shows the second relaxation in quick succession; the absence of this relaxation with both sPSF and sPEK may be due to the lack of side-chain (Figure 5). Hence, the  $\gamma$  relaxation in the Nafion may be originating from the side-chain holding the  $-\text{SO}_3\text{H}$  group.

**Figure 7** shows the  $\gamma$  relaxation within Nafion-117 in the temperature range of  $-100$ – $20^\circ\text{C}$ . Di Noto *et al.* observed a relaxation in the same temperature range and attributed it to the relaxation of the ether side-chain bound to  $-\text{SO}_3\text{H}$ .<sup>39</sup> The relaxation peak enters the frequency window at  $100^\circ\text{C}$  at a frequency of 0.1 Hz and it quickly moves towards the HF region (10 kHz) as the temperature is increased to  $-40^\circ\text{C}$ . However, above  $50^\circ\text{C}$ , a reversal in the peak movement is observed as the  $\gamma$  relaxation peak shifts towards lower frequencies, and there is a significant rise in the  $\Delta\epsilon$  value upto a temperature of  $170^\circ\text{C}$  (Figure 7b). This shift towards lower frequencies may be attributed to the water-loss and the subsequent packing of the chains, which restricts the motion of side-chains.

### < Figure 7 >

The relaxation peak movement depends on several factors *viz.* chain stacking, morphology, type of polymer (Type A, B and C) dipole orientation *etc.* However, further studies need to be carried out to ascertain the reason for the increase in the dielectric loss and the consequent peak shift to lower frequencies with temperature.

Since only limited reports are available on the BDS of polyether ketones (especially PEEK) it is challenging to assign the intermediate relaxation (peaks other than  $\zeta$  and  $\delta$  relaxations).<sup>71-74</sup> The  $\gamma$  and  $\beta$  relaxations in sPEK are shown in **Figure 8**; the origin of the  $\gamma$  relaxation is attributed to the rotational mobility of phenylene ring and it is reported that the mobility of phenyl group between the ether-ether link is higher when compared to that between ether-ketone.<sup>71-74</sup> David *et al.* attributed the  $\gamma$  relaxation to the crankshaft motion of isolated chain portion using dynamical mechanical spectroscopy and molecular dynamic simulation.<sup>71</sup> Therefore, based on the appearance of the relaxation peak and the comparable activation energy as that reported in the literature, the  $\gamma$  relaxation can be proposed to be arising from the crankshaft motion associated with the ether linkage of the main-chain.

### < Figure 8 >

#### *Relaxations above 20°C*

##### **(d) $\beta$ relaxation**

The backbone related motion of all the three membranes (Nafion-117, sPSF and sPEK) has been assigned as the  $\beta$  relaxation. **Figure 9** shows the  $\beta$  relaxation assigned to the fluctuation of the dipole moment of the ether side-chain attached to the backbone of the Nafion-117.<sup>39</sup>  $\beta$  relaxation enters the frequency window at -80°C onwards (at ~0.1 Hz) and by ~20°C the peak shifts to

higher frequencies (~10 Hz) (Figure 9a). From 20 to 180°C, the  $\beta$  relaxation continues to shift to higher frequency and this can be explained based on the thermal activation of the chain movement (Figure 9b). The increase in dielectric strength with temperature is expected as more number of polymer chains participates in the relaxation process (Figure S14).

< **Figure 9** >

The  $\beta$  relaxation in sPSF membrane in the temperature range of -20 – 180°C is shown in **Figure 10**. A very low intensity peak is observed at -20°C at a frequency of 0.5 Hz which gradually shifts towards higher frequency (~50 Hz), and there is an exponential rise in the peak intensity upto a temperature of 70°C. Above 80°C, the peak shifts to lower frequencies with simultaneous decrease in the peak intensity. Similar to the observation with  $\gamma$  relaxation of Nafion-117, the reversal in peak movement can be attributed to the water loss and the consequent chain packing. Tsuwi *et al.* attributed the  $\beta$  relaxation in SF-PSF at a frequency of 100 Hz (at 80°C) to the backbone motion of the polymer.<sup>49</sup> The high activation energy of this relaxation, ~72 kJ mol<sup>-1</sup>, is attributed to the non-local fluctuations and packaging defects in the material. However, with sPSF, the  $E_A$  of  $\beta$  relaxation is 51.12 kJ mol<sup>-1</sup>, and it varies from PSF depending on the attached side-group (SF, -COOH etc.)<sup>49</sup>

< **Figure 10** >

The  $\beta$  relaxation with sPEK is also known as sub-glass transition relaxation and it originates from localized motion in the bulk and organized regions of the amorphous phase (Figure 8b). The transformation from amorphous to semi-crystallinity causes a decrease in the dielectric strength of  $\beta$  relaxation in sPEK. At -30°C, the relaxation appears at a frequency of 0.2 Hz and it shifts to higher frequency with temperature. Beyond 40°C, the dielectric strength starts to

decrease significantly with increase in temperature. With a high  $E_A$  of  $49.78 \text{ kJ mol}^{-1}$ , this relaxation is assigned to the rotational motion of the main-chain. The activation energy of the  $\beta$  relaxation in Nafion-117 is slightly higher ( $60.48 \text{ kJ mol}^{-1}$ ) than those of the sPSF and sPEK membranes; this might be attributed to the slower chain ( $-\text{CF}_2-$  backbone) motion in the dehydrated membrane.

#### **(e) $\alpha$ relaxation**

With Nafion-117, the relaxation peak which enters the frequency window at temperature above  $130^\circ\text{C}$  (Figure 9c) is related to the dynamic glass-transition or the  $\alpha$  relaxation; with increase in temperature the relaxation peak shifts to higher frequency. The  $\alpha$  relaxation temperature is in line with the  $T_g$  of  $\sim 152^\circ\text{C}$  measured from the DSC thermograms (Figure S15). The  $T_g$  of Nafion-117 is reported to be in the temperature range of  $100$ – $160^\circ\text{C}$  depending on the water content in the membrane.<sup>75,76</sup> The  $\Delta\varepsilon$  of  $\alpha$  relaxation is almost constant with further increase in temperature. With sPSF, a fourth relaxation peak appears at a temperature of  $\sim 180^\circ\text{C}$ , but it is completely eclipsed by the high intensity of the dielectric loss. This relaxation can be clearly observed in the  $\text{Tan } \delta$  plot (Figure 3b). Bare PSF shows a  $T_g$  of  $\sim 186^\circ\text{C}$ , whereas, after sulfonation a significant increase in  $T_g$  is observed ( $217^\circ\text{C}$ , Figure S15). The reported glass transition temperature range of  $180$  –  $220^\circ\text{C}$  with polysulfone-based materials (PSF, sPSF, SF-PSF and COOH-PSF) indicates that this peak corresponds to the primary relaxation ( $\alpha$ ).<sup>49,77</sup> The intensity of dielectric loss beyond  $160^\circ\text{C}$  (Figure S8d) is considerably higher when compared to that at lower temperatures due to very high electrode and interfacial polarization. These factors mask the features due to relaxation and therefore it is extremely difficult to fit the data using HN equation at high temperatures.

## CONCLUSIONS

Nafion-117, sulfonated polysulfone (sPSF) and sulfonated polyetherketone (sPEK) were characterized using broadband dielectric spectroscopy (BDS) to investigate the effect of water content and sulfonation on the polymer relaxations. An optimum ac amplitude ( $\sim 100$  mV<sub>rms</sub>) was used to minimize the contributions from the interfacial/electrode polarizations in the low frequency region.

With all the three membranes, a broad relaxation peak of low dielectric strength is observed in the temperature range of  $\sim -130 - -80^\circ\text{C}$ . This relaxation ( $\zeta$ ) in the mid-frequency region is attributed to the confined water in the membrane. The activation energy values reported in the literature for the relaxation of confined-water in various dielectric materials (polymers, organic and inorganic systems) support this peak assignment. But, it is seldom reported with PEMs perhaps due to the low dielectric strength of the relaxation process; the use of 1 V ac amplitude causes high electrode polarization and hence eclipses this feeble peak. The second relaxation peak ( $\delta$ ) in the same temperature and frequency ranges is attributed to the  $-\text{SO}_3\text{H}$  group. The negligible dielectric strength of this relaxation process with sPEK of low degree of sulfonation confirms this assignment. With Nafion, a third relaxation peak ( $\gamma$ ) is observed in the temperature range of  $-90 - 170^\circ\text{C}$  related to the motion of the side-chain; this particular relaxation is missing with the other two polymers without the side-chain. The  $\beta$  relaxation is observed with all the three membranes but at different temperature ranges; with sPSF and sPEK, the  $\beta$  relaxation shows comparable activation energy values due to the similar backbone (phenyl rings in the main-chain). The  $\alpha$  relaxation due to the glass transition could only be observed with Nafion-117 at  $\sim 150^\circ\text{C}$  (frequency of  $\sim 1$  Hz), whereas, it is hardly discernible with sPSF and sPEK membranes. All the relaxation peaks are confirmed from the  $\text{Tan } \delta$  and dielectric loss plots.

## SUPPORTING INFORMATION

Additional supporting information may be found in the online version of this article.

## ACKNOWLEDGEMENTS

Department of Science and Technology (DST), India is acknowledged for the financial support of the research work through the grant SR/S1/PC-68/2012. MEMS department at IIT Bombay is acknowledged for providing the broadband dielectric spectroscopy (BDS) facility.

## REFERENCES

1. Kremer, F.; Schönhals, A. In *Broadband Dielectric Spectroscopy*, Springer-Verlag Berlin Heidelberg GmbH, **2002**.
2. Sengers, W. G. F., van den Berg, O., Wübbenhorst, M., Gotsis, A. D. and Picken, S. J., *Polymer* **2005**, *46*, 6064–6074.
3. Vassilikou-dova, A.; Kalogeras, I. M. In *Dielectric Analysis (DEA)- Thermal Analysis of Polymers: Fundamental Applications*, John Wiley & Sons, Inc. New York, **2009**, 497–613.
4. Cosby, T., Holt, A., Griffin, P. J., Wang, Y. and Sangoro, J. *J. Phys. Chem. Lett.* **2015**, *6*, 3961–3965.
5. Santos, L. D., Dubrunfaut, O., Badot, J.-C. and Laberty-Robert, C. *J. Phys. Chem. C* **2016**, *120*, 6963–6970.
6. Di Noto, V., Piga, M., Giffin, G. A. and Pace, G. *J. Memb. Sci.* **2012**, *390*, 58–67.
7. Konnertz, N., Ding, Y., Harrison, W. J., Budd, P. M. and Schönhals, A. *ACS Macro Lett.* **2016**, *5*, 528–532.

8. Lin, Y., Tan, Y., Qiu, B., Cheng, J., Wang, W., Shangguan, Y. and Zheng, Q. *J. Memb. Sci.* **2013**, *439*, 20–27.
9. Redondo-Foj, B., Carsi, M., Ortiz-Serna, P., Sanchis, M. J., Darcia, F. and Garcia, J. M. *J. Phys. D: Appl. Phys.* **2013**, *46*, 295304 (12pp).
10. Nayak, L., Khastgir, D. and Chaki, T. K. *Polym. Compos.* **2012**, *33*, 85–91.
11. Tarnacka, M., Dulski, M., Starzonek, S., Adrjanowicz, K., Mapesa, E. U., Kaminski, K. and Paluch, M. *Polymer* **2015**, *68*, 253–261.
12. Di Noto, V., Piga, M., Giffin, G. A., Lavina, S., Smotkin, E. S., Sanchez, J.-Y. and Iojoiu, C. *J. Phys. Chem. C* **2012**, *116*, 1370–1379.
13. Sood, R., Zhang, B., Serghei, A., Bernard, J. and Drockenmuller, E. *Poly. Chem.* **2015**, *6*, 3521–3528.
14. Wojnarowska, Z. and Paluch, M. *J. Phys.: Condens. Matter* **2015**, *27*, 073202 (20pp).
15. Kreuer, K. D. *J. Memb. Sci.* **2001**, *185*, 29–39.
16. Neergat, M., Seiler, T., Savinova, E. R. and Stimming, U., *J. Electrochem. Soc.* **2006**, *153*, A997–A1003.
17. Cappadonia, M., Erning, J. W. and Stimming, U. *J. Electroanal. Chem.* **1994**, *376*, 189–193.
18. Saito, M., Hayamizu, K. and Okada, T. *J. Phys. Chem. B.* **2005**, *109*, 3112–3119;
19. Mukundan, R., Kim, Y. S., Garzon, F. and Pivovar, B. *ECS Transactions*, **2006**, *1*, 403–413.
20. Wang, F., Hickner, M., Seung, Y., Zawodzinski, T. A. and Mcgrath, J. E. *J. Memb. Sci.*, **2002**, *197*, 231–242.

21. Klaysom, C., Ladewig, B. P., Lu, G. Q. M. and Wang, L. *J. Memb. Sci.* **2011**, 368, 48–53.
22. Xing, P., Robertson, G. P., Guiver, M. D., Mikhailenko, S. D., Wang, K. and Kaliaguine, S. *J. Memb. Sci.* **2004**, 229, 95–106.
23. Zhang, G., Fu, T., Wu, J., Li, X. and Na, H. *J. Appl. Polym. Sci.* **2010**, 116, 1515–1523.
24. Zhang, Y., Wan, Y., Zhang, G., Shao, K., Zhao, C., Li, H. and Na, H. *J. Memb. Sci.* **2010**, 348, 353–359.
25. Kim, J. and Kim, D. *J. Memb. Sci.* **2012**, 405-406, 176–184.
26. Zhou, S. and Kim, D. *Electrochim. Acta* **2012**, 63, 238–244.
27. Zhu, M., Song, Y., Hu, W., Li, X., Jiang, Z., Guiver, M. D. and Liu, B. *J. Memb. Sci.* **2012**, 1, 520–526.
28. Saxena, P., Gaur, M. S., Shukla, P. and Khare, P. K. *J. Electrostat.* **2008**, 66, 584–588.
29. Zawodzinski Jr., T. A., Neeman, M., Sillerud, L. O. and Gottesfeld, S. *J. Phys. Chem.* **1991**, 95, 6040–6044.
30. Zawodzinski Jr., T. A., Derouin, C., Radzinski, S., Sherman, R. J., Smith, V. T., Springer, T. E. and Gottesfeld, S. *J. Electrochem. Soc.* **1993**, 140, 1041–1047.
31. Bose, S., Kuila, T., Nguyen, T. X. H., Kim, N. H., Lau, K. and Lee, J. H. *Prog. Polym. Sci.*, **2011**, 36, 813–843.
32. Tsonos, C., Apekis, L. and Pissis, P. *J. Mater. Sci.* **1998**, 33, 2221–2226.
33. Paddison, S. J., Reagor, D. W. and Zawodzinski Jr., T. A. *J. Electroanal. Chem.* **1998**, 459, 91–97.
34. Di Noto, V., Piga, M., Lavina, S., Negro, E., Yoshida, K., Ito, R. and Furukawa, T. *Electrochim. Acta* **2010**, 55, 1431–1444.



35. Di Noto, V., Gliubizzi, R., Negro, E. and Pace, G. *J. Phys. Chem. B* **2006**, *110*, 24972–24986.
36. Rhoades, D. W., Hassan, M. K., Osborn, S. J., Moore, R. B. and Mauritz, K. A. *J. Power Sources* **2007**, *172*, 72–77.
37. Di Noto, V., Piga, M., Pace, G., Negro, E. and Lavina, S. *ECS Trans.* **2008**, *16*, 1183–1193.
38. Mauritz, K. A. and Hassan, M. K. *ECS Trans.* **2009**, *25*, 371–384.
39. Di Noto, V.; Negro, E.; Lavina, S. In *Fuel Cell Chemistry and Operation: ACS Symposium Series*; American Chemical Society: Washington, DC, **2010**.
40. Di Noto, V., Boaretto, N., Negro, E., Stallworth, P. E., Lavina, S., Giffin, G. A., Greenbaum, S. G. and Marzolo, V. *Int. J. Hydrogen Energy* **2011**, *37*, 6215–6227.
41. Hassan, M. K., Abukmail, A. and Mauritz, K. A. *Eur. Polym. J.* **2012**, *48*, 789–802.
42. Di Noto, V., Piga, M., Giffin, G. A., Vezzù, K. and Zawodzinski, T. A. *J. Am. Chem. Soc.* **2012**, *134*, 19099–19107.
43. Giffin, G. A., Piga, M., Lavina, S., Navarra, M. A., Epifanio, A. D., Scrosati, B. and Di Noto, V. *J. Power Sources* **2012**, *198*, 66–75.
44. Matos, B. R., Dresch, M. A., Santiago, E. I., Linardi, M., De Florio, D. Z. and Fonseca, F. C. *J. Electrochem. Soc.* **2013**, *160*, 43–48.
45. Matos, B. R., Santiago, E. I., Rey, J. F. Q. and Fonseca, F. C. *Phys. Rev. E* **2014**, *89*, 052601–052607.
46. Deng, Z. D. and Mauritz, K. A. *Macromolecules* **1992**, *25*, 2739–2745.
47. Chen, R. S., Jayakody, J. P., Greenbaum, S. G., Park, Y. S., Xu, G., McLin, M. G. and Fontanella, J. J. *J. Electrochem. Soc.* **1993**, *140*, 889–895.

48. Di Noto, V.; Giffin, G. A.; Vezzu, K.; Piga, M.; Lavina, S. In *Solid State Proton Conductors: Properties and Applications in Fuel Cells*, John Wiley & Sons, Inc. New York, **2012**.
49. Tsuwi, J., Pospiech, D., Jehnichen, D., Ha, L. and Kremer, F. *J. Appl. Polym. Sci.* **2007**, *105*, 201–207.
50. Labahn, D., Mix, R. and Schönhals, A. *Phys. Rev. E*, **2009**, *79*, 011801–011809.
51. Soboleva, T., Xie, Z., Shi, Z., Tsang, E., Navessin, T. and Holdcroft, S. *J. Electroanal. Chem.* **2008**, *622*, 145–152.
52. Noshay, A. and Robeson, L. M. *J. Appl. Polym. Sci.* **1976**, *20*, 1885–1903.
53. Guan, R., Zou, H., Lu, D., Gong, C. and Liu, Y. *Eur. Polym. J.* **2005**, *41*, 1554–1560.
54. Mauritz, K. A. and Moore, R. B. *Chem. Rev.*, **2004**, *104*, 4535–4585.
55. Peckham, T. J. and Holdcroft, S. *Adv. Mater.* **2010**, *22*, 4667–469.
56. Peron, J., Mani, A., Zhao, X., Edwards, D., Adachi, M., Soboleva, T., Shi, Z., Xie, Z., Navessin, T. and Holdcroft, S. *J. Memb. Sci.* **2010**, *356*, 44–51.
57. Yang, J. and Brown, P. J. *Chinese J. Polym. Sci.* **2008**, *26*, 263–273.
58. Korbakov, N., Harel, H., Feldman, Y. and Marom, G. *Chem. Phys.* **2002**, *203*, 2267–2272.
59. Atornjitjawat, P., Pipatpanyanugoon, K. and Aree, T. *Poly. Adv. Technol.* **2014**, *25*, 1027–1033.
60. S. Cervený, G. A. Schwartz, R. Bergman, J. Swenson, *Phys. Rev. Lett.* **2004**, *93*, 245702–4.
61. Faraone, A., Liu, L., Mou, C.-Y., Yen, C.-W. and Chen, S.-H. *J. Chem. Phys.* **2004**, *121*, 10843–10846.

62. Swenson, J., Jansson, H. and Bergman, R. *Phys. Rev. Lett.* **2006**, *96*, 247802–4.
63. Laurati, M., Sotta, P., Long, D. R., Fillot, L.-A., Arbe, A., Algria, A., Embs, J. P., Unruh, T., Schneider, G. J. and Colmenero, J. *Macromolecules* **2012**, *45*, 1676–1687.
64. Swenson, J. and Cerveny, S. *J. Phys.: Condens. Matter* **2015**, *27*, 033102.
65. Li, X.-F., Paoloni, F. P. V., Weiber, E. A., Jiang, Z.-H. and Jannasch, P. *Macromolecules*, **2012**, *45*, 1447–1459.
66. Jutemar, E. P. and Jannasch, P. *J. Memb. Sci.*, **2010**, *351*, 87–95.
67. Yee, A. F. and Smith, S. A. *Macromolecules* **1981**, *14*, 54–64.
68. Varadarajan, K. and Boyer, R. F. *J. Poly. Sci. Poly. Phys. Ed.* **1982**, *20*, 141–154.
69. Aitken, C. L., McHattie, J. S. and Paul, D. R. *Macromolecules* **1992**, *25*, 2910–2922.
70. Leonardi, A., Dantras, E., Dandurand, J. and Lacabanne, C. *J. Therm. Anal. Calorim.* **2013**, *111*, 807–814.
71. David, L., Girard, C., Dolmazon, R., Albrand, M. and Etienne, S. *Macromolecules* **1996**, *29*, 8343–8348.
72. Kalika, D. S. and Krishnaswamy, R. K. *Macromolecules* **1993**, *26*, 4252–4261.
73. Nogales, A., Ezquerro, T. A., Batallan, F., Frick, B., Lopez-Cabarcos, E. and Balta-Calleja, F. J. *Macromolecules* **1999**, *32*, 2301–2308.
74. Verot, S., Battesti, P. and Perrier, G. *Polymer* **1999**, *40*, 2605–2617.
75. Cho, K.-Y., Jung, H.-Y., Sung, K. A., Kim, W.-K., Sung, S.-J., Park, J.-K., Choi, J.-H. and Sung, Y.-E. *J. Power Sources* **2006**, *159*, 524–528.
76. Osborn, S. J., Hassan, M. K., Divoux, G. M., Rhoades, D. W., Mauritz, K. A. and Moore, R. B. *Macromolecules* **2007**, *40*, 3886–3890.
77. Diogo, H. P. and Ramos, J. J. M. *J. Therm. Anal. Calorim.* **2013**, *111*, 773–779.

## FIGURE CAPTIONS

**Figure 1** Chemical structures of Nafion (a), sulfonated polysulfone (sPSF) (b), sulfonated polyetheretherketone (sPEEK) (c), and sulfonated polyetherketone (sPEK) (d).

**Figure 2** Dielectric loss ( $\epsilon''$ ) as a function of frequency and temperature with membranes of Nafion-117 (a), sPSF (b), and sPEK (c).

**Figure 3**  $\tan \delta$  as a function of temperature at a frequency of 1.355 Hz with membranes of Nafion-117 (a), sPSF (b), and sPEK (c). Inset to (c) shows the magnified view of the  $\zeta$  relaxation in sPEK.

**Figure 4** Dielectric loss ( $\epsilon''$ ) of Nafion-117 membrane at a temperature of  $-40^\circ\text{C}$  (a) and  $10^\circ\text{C}$  (b) fitted with 3 HN functions.

**Figure 5** Dielectric loss ( $\epsilon''$ ) at different temperatures with membranes of Nafion-117 (a), sPSF (b), and sPEK (c); the arrows show the movement of the relaxation peaks to higher frequency with temperature.

**Figure 6** Dielectric loss ( $\epsilon''$ ) at different temperatures with membranes of Nafion-117 (a), sPSF (b), and sPEK (c); the arrows show the movement of the relaxation peaks to higher frequency with temperature.

**Figure 7** The variation in dielectric loss ( $\epsilon''$ ) and the relaxation peak shift with frequency for  $\gamma$  relaxation of Nafion-117 membrane in the low temperature range (a), and high temperature range (b). The arrows indicate the movement of the relaxation peaks and the change in intensity of  $\epsilon''$ .

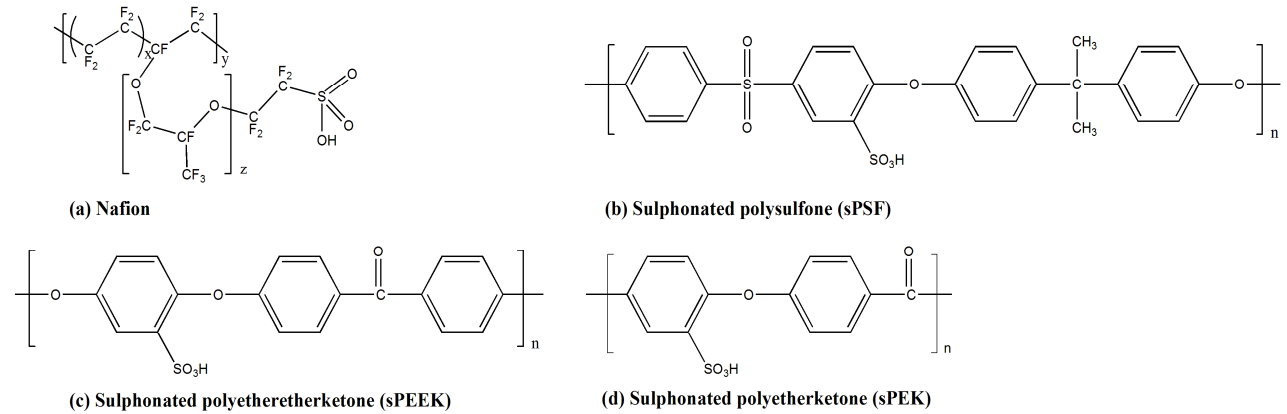
**Figure 8** The variation in dielectric loss ( $\epsilon''$ ) and the relaxation peak shift with frequency for  $\gamma$  (a) and  $\beta$  (b) relaxations with sPEK membrane at different temperatures.

**Figure 9** The variation in dielectric loss ( $\epsilon''$ ) and the relaxation peak shift with frequency for  $\beta$  relaxation in the low temperature range (a),  $\beta$  relaxation in the high temperature range (b), and  $\alpha$  relaxation (c) with Nafion-117 membrane. Inset to (a) shows the magnified view of the appearance of  $\beta$  relaxation. The arrows indicate the movement of the relaxation peaks and the change in intensity of  $\epsilon''$ .

**Figure 10** The variation in dielectric loss ( $\epsilon''$ ) and the peak shift with frequency for  $\beta$  relaxation towards HF region (a) and LF region (b) with sPSF membrane at different temperatures. The upward and downward arrows shows the trends in the relaxation peak movement.

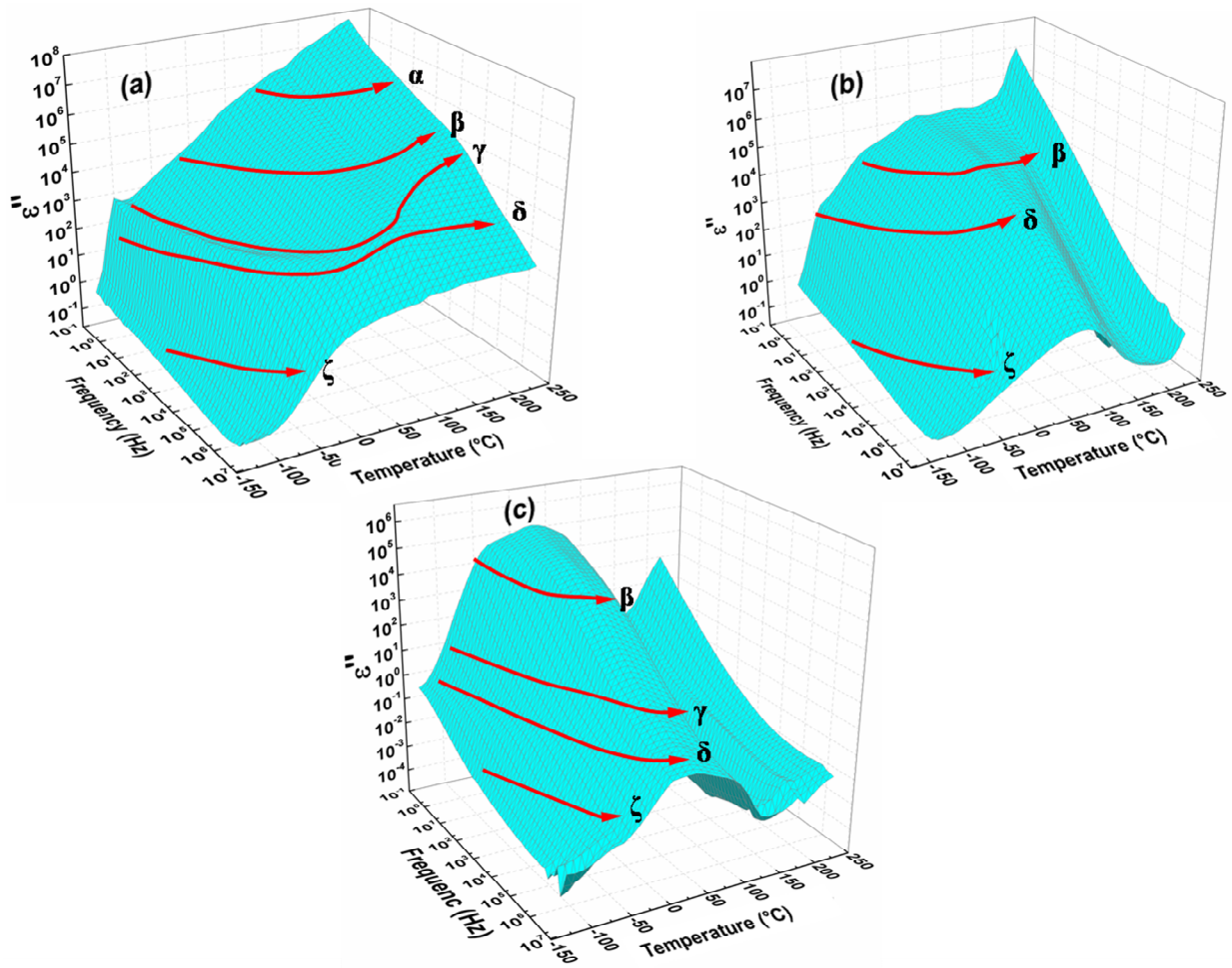
## FIGURES

**Figure 1**



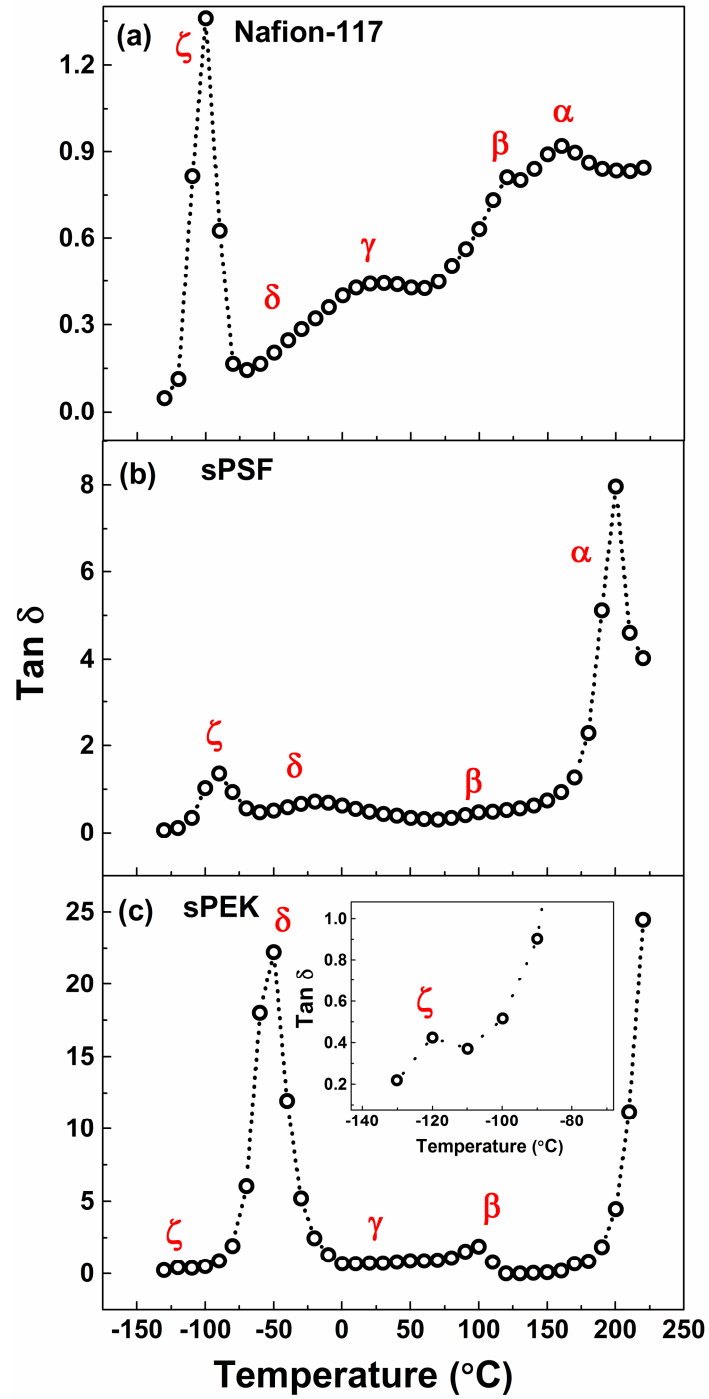
Chemical structures of Nafion (a), sulfonated polysulfone (sPSF) (b), sulfonated polyetheretherketone (sPEEK) (c), and sulfonated polyetherketone (sPEK) (d).

Figure 2



Dielectric loss ( $\epsilon''$ ) as a function of frequency and temperature with membranes of Nafion-117 (a), sPSF (b), and sPEK (c).

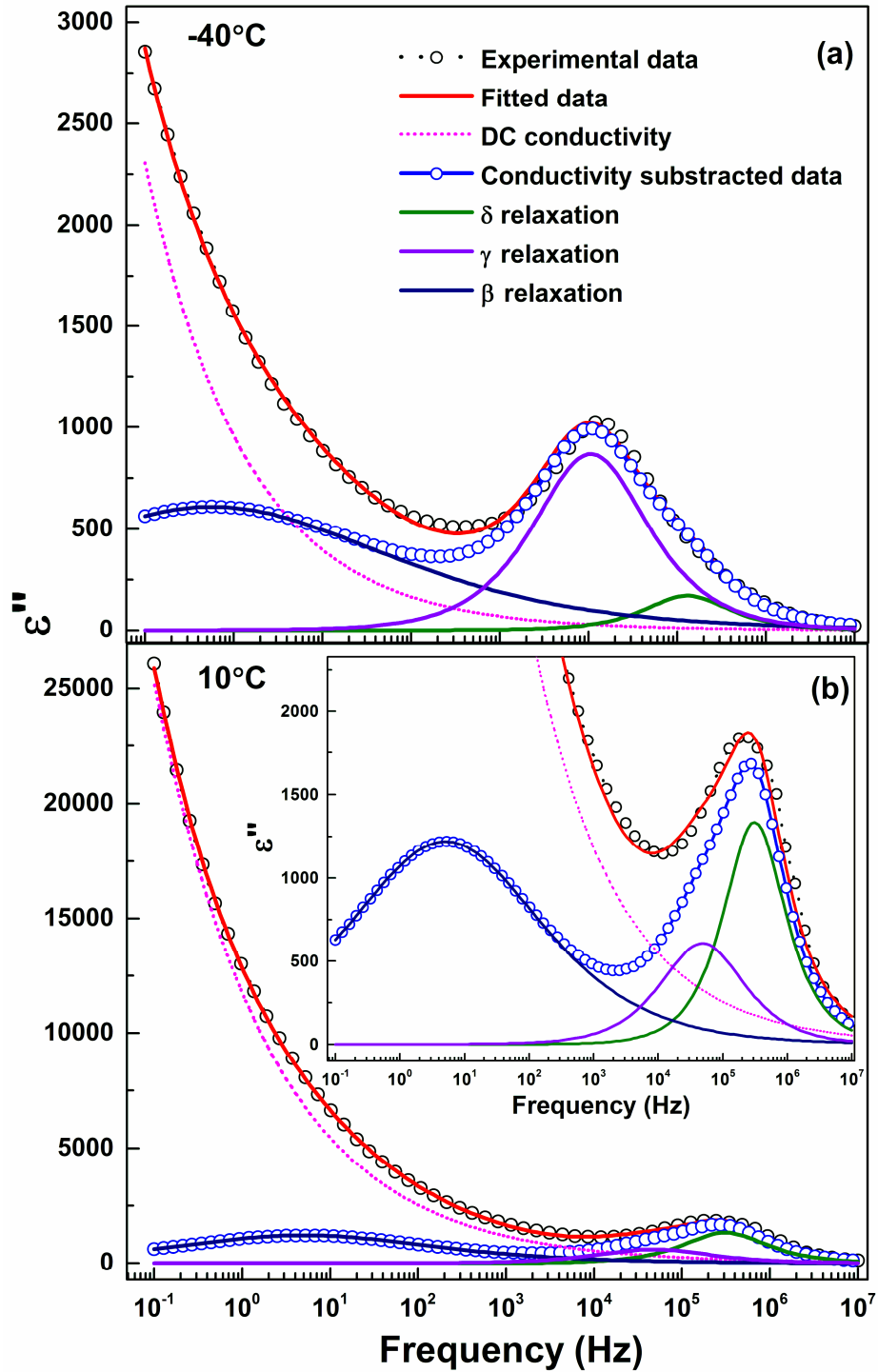
Figure 3



$\tan \delta$  as a function of temperature at a frequency of 1.355 Hz with membranes of Nafion-117 (a), sPSF (b), and sPEK (c). Inset to (c) shows the magnified view of the  $\zeta$  relaxation in sPEK.

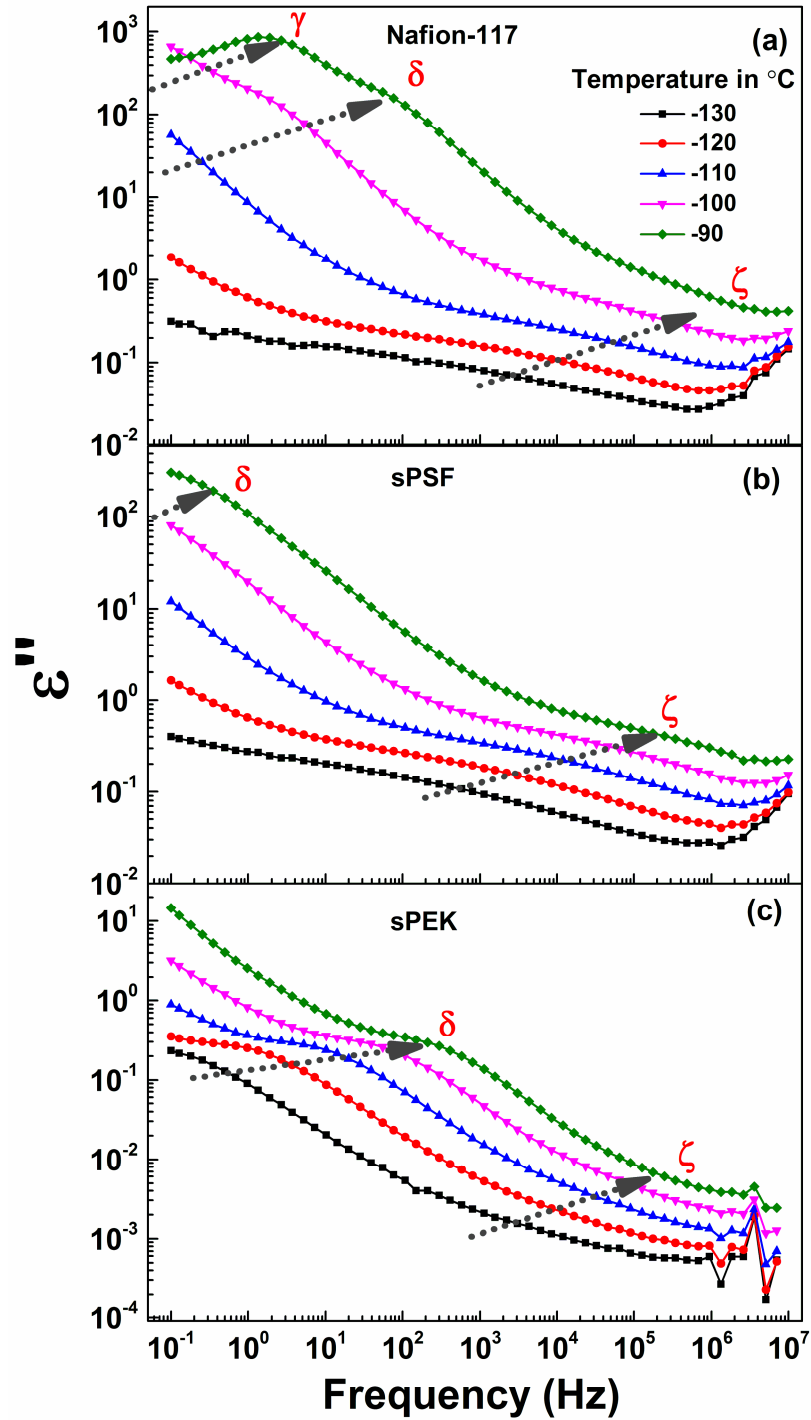


Figure 4



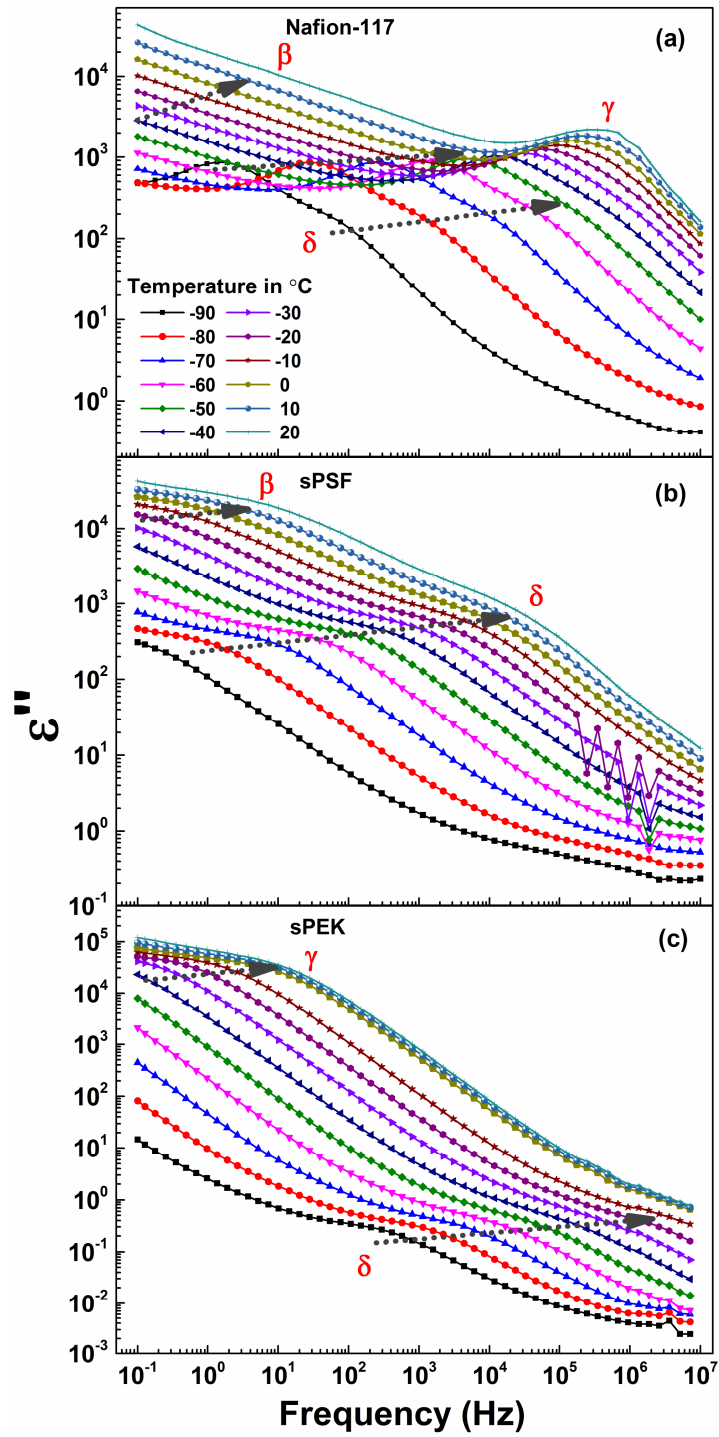
Dielectric loss ( $\epsilon''$ ) of Nafion-117 membrane at a temperature of  $-40^\circ\text{C}$  (a) and  $10^\circ\text{C}$  (b) fitted with 3 HN functions.

Figure 5



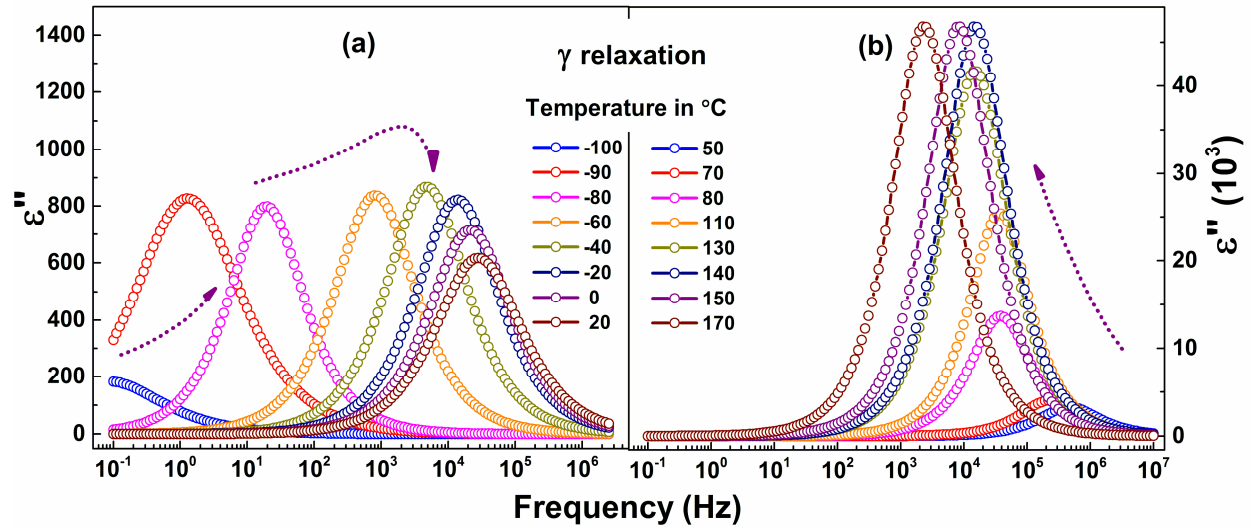
Dielectric loss ( $\epsilon''$ ) at different temperatures with membranes of Nafion-117 (a), sPSF (b), and sPEK (c); the arrows show the movement of the relaxation peaks to higher frequency with temperature.

Figure 6



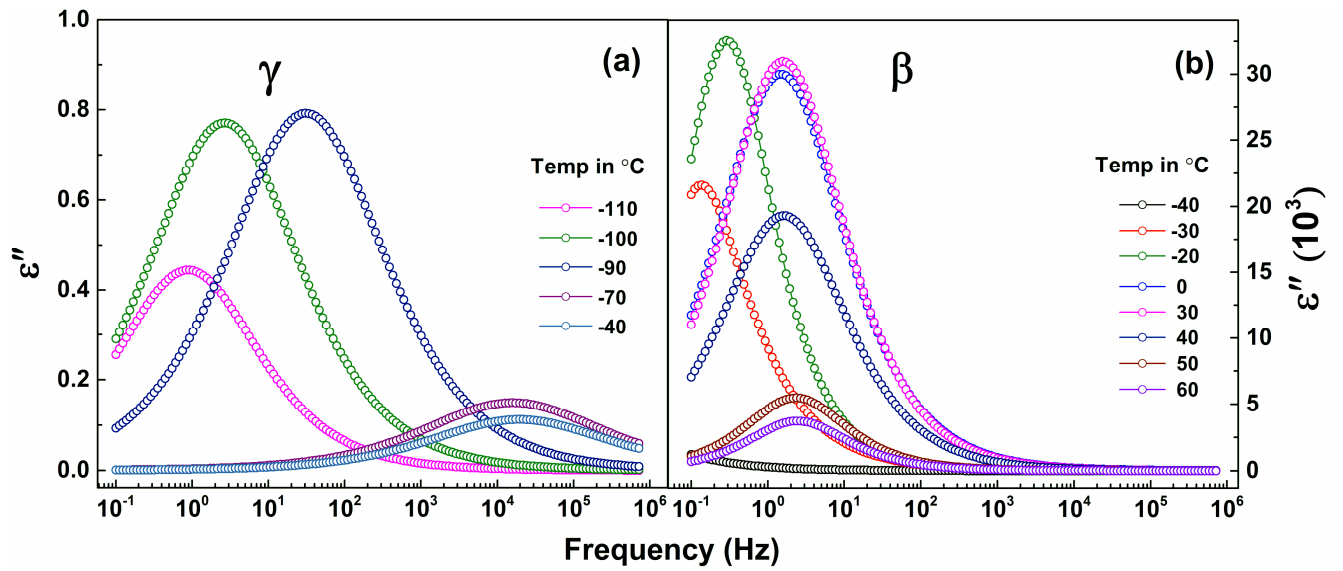
Dielectric loss ( $\epsilon''$ ) at different temperatures with membranes of Nafion-117 (a), sPSF (b), and sPEK (c); the arrows show the movement of the relaxation peaks to higher frequency with temperature.

Figure 7



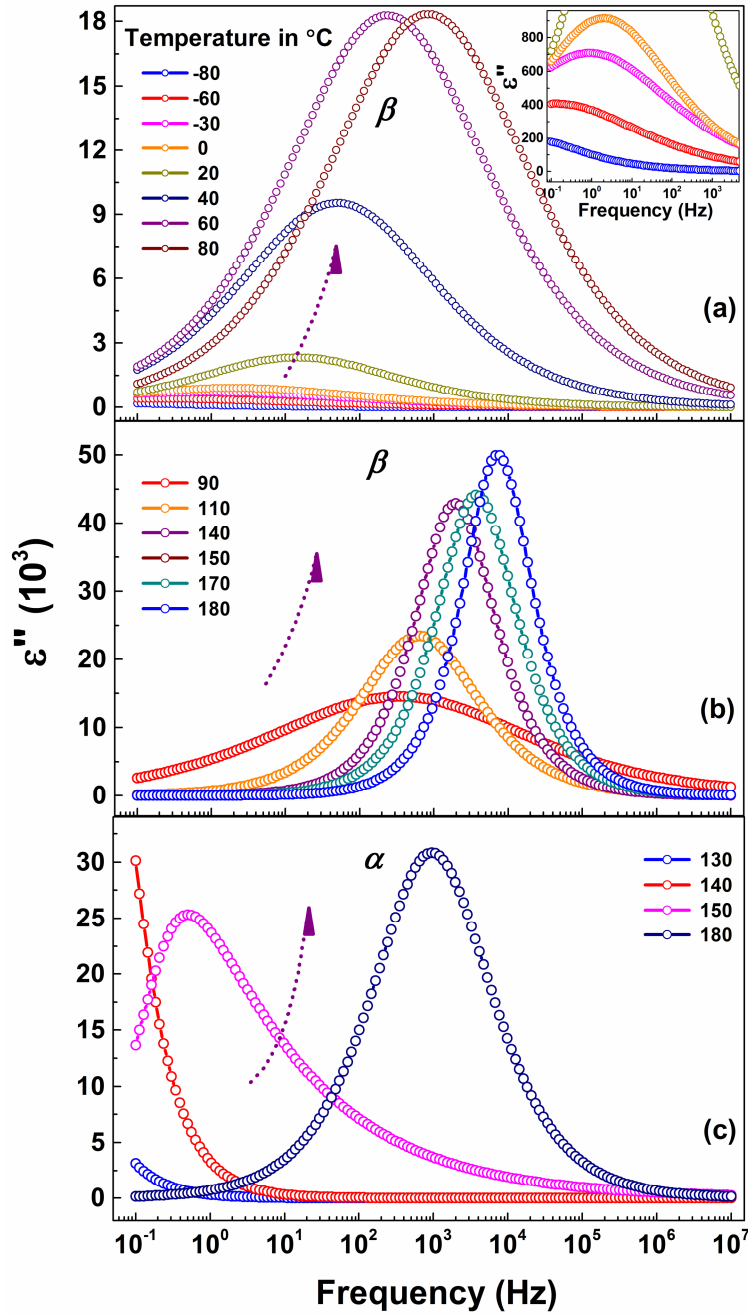
The variation in dielectric loss ( $\epsilon''$ ) and the relaxation peak shift with frequency for  $\gamma$  relaxation of Nafion-117 membrane in the low temperature range (a), and high temperature range (b). The arrows indicate the movement of the relaxation peaks and the change in intensity of  $\epsilon''$ .

Figure 8



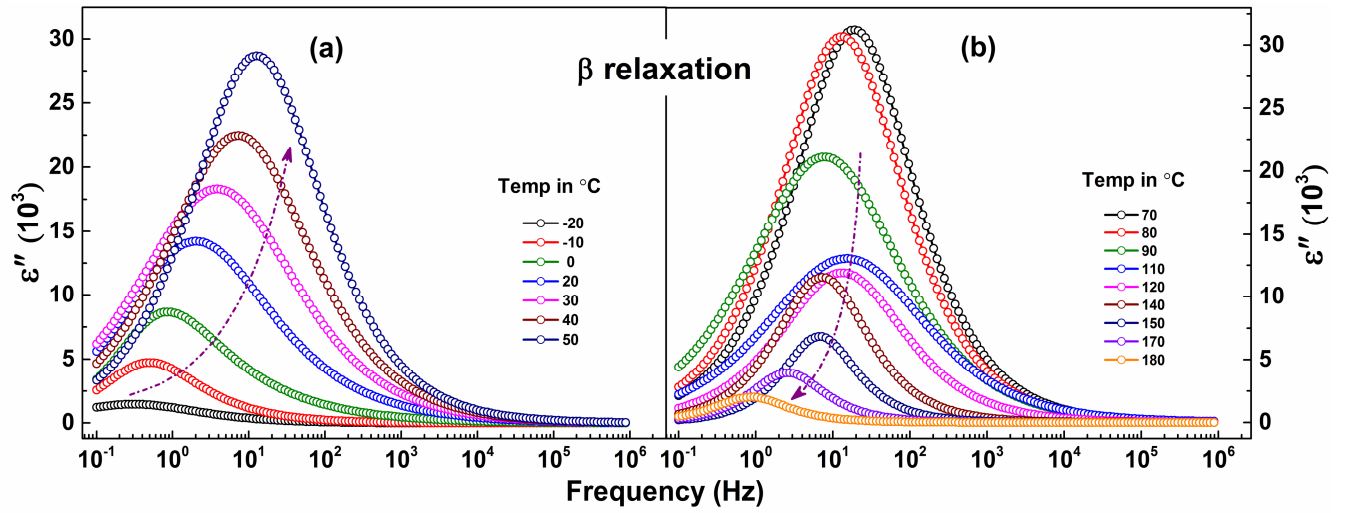
The variation in dielectric loss ( $\epsilon''$ ) and the relaxation peak shift with frequency for  $\gamma$  (a) and  $\beta$  (b) relaxations with sPEK membrane at different temperatures.

Figure 9



The variation in dielectric loss ( $\epsilon''$ ) and the relaxation peak shift with frequency for  $\beta$  relaxation in the low temperature range (a),  $\beta$  relaxation in the high temperature range (b), and  $\alpha$  relaxation (c) with Nafion-117 membrane. Inset to (a) shows the magnified view of the appearance of  $\beta$  relaxation. The arrows indicate the movement of the relaxation peaks and the change in intensity of  $\epsilon''$ .

Figure 10



The variation in dielectric loss ( $\epsilon''$ ) and the peak shift with frequency for  $\beta$  relaxation towards HF region (a) and LF region (b) with sPSF membrane at different temperatures. The upward and downward arrows shows the trends in the relaxation peak movement.

**Table 1.** Ion exchange capacity and degree of sulfonation of the membranes

<b>Membrane</b>	<b>Water content (%)</b>	<b>Ion exchange capacity (m equiv)</b>	<b>Degree of sulfonation (%)</b>
Nafion-117	18	1.15	-
sPSF	14	1.22	62
sPEK	13	0.08	6



## Supporting Information

### Broadband dielectric spectroscopy of Nafion-117, sulfonated polysulfone (sPSF) and sulfonated polyether ketone (sPEK) membranes

Wasim F. G. Saleha<sup>1,2</sup>, Rahul Ramesh<sup>2</sup>, Nalajala Naresh<sup>1,2</sup>, Arup Chakraborty<sup>2</sup>, Bradley P. Ladewig<sup>3</sup> and Manoj Neergat<sup>2,\*</sup>

<sup>1</sup>IITB-Monash Research Academy, Powai, Mumbai, India-400076

<sup>2</sup>Department of Energy Science and Engineering, Indian Institute of Technology Bombay (IITB), Mumbai, India-400076

<sup>3</sup>Department of Chemical Engineering, Imperial College London, Exhibition Road, London SW7 2AZ, United Kingdom

\*Corresponding author. Tel.: +91 22 2576 7893; Fax: +91 22 2576 4890

E-mail address: [nmanoj@iitb.ac.in](mailto:nmanoj@iitb.ac.in)

#### 1. Ion exchange capacity (IEC), water absorption and degree of sulfonation

The membrane samples were first dried in an oven at 80°C for 24 h and its weight was noted down as  $W_D$ . The membranes were kept in 1 M HCl for 24 h to obtain their acid form and washed repeatedly with DI water to remove the excess acid. These membranes were immersed in 1 M NaCl for 24 h to liberate the  $H^+$  ions ( $H^+$  ions replaced with  $Na^+$  ions). The solution was titrated with 0.01 M NaOH using phenolphthalein indicator and the IEC was calculated using the following formula:

$$IEC = \frac{\text{consumed ml of NaOH} \times \text{molarity of NaOH}}{\text{dry weight of the membrane}}$$

To calculate the water uptake capacity, the membranes were dried in an oven overnight and the accurate weight was recorded as  $W_D$ . The samples were kept in DI water for 1 day, the wet membranes were wiped with a tissue paper, and the weight was noted as  $W_W$ . The membrane seemed to have absorbed the maximum water in a day itself as the weight of the wet membrane remained same even after a week of immersion in the DI water. The water uptake of the membrane was calculated using the following formula:

$$\text{Water uptake} = (W_W - W_D)/W_D$$

where,  $W_W$  and  $W_D$  are the weights of wet and dry membranes, respectively.

The degree of sulfonation for sPSF was calculated from the titration values using the following formula:

$$DS = \frac{0.442[M(\text{NaOH}) \times V(\text{NaOH})]}{W_D - 0.081[M(\text{NaOH}) \times V(\text{NaOH})]}$$

where,  $M$  (NaOH) and  $V$  (NaOH) are the molarity and the volume of the NaOH, respectively; the molecular weight of the polysulfone monomer unit and sulfonic group are 441 and 81, respectively.

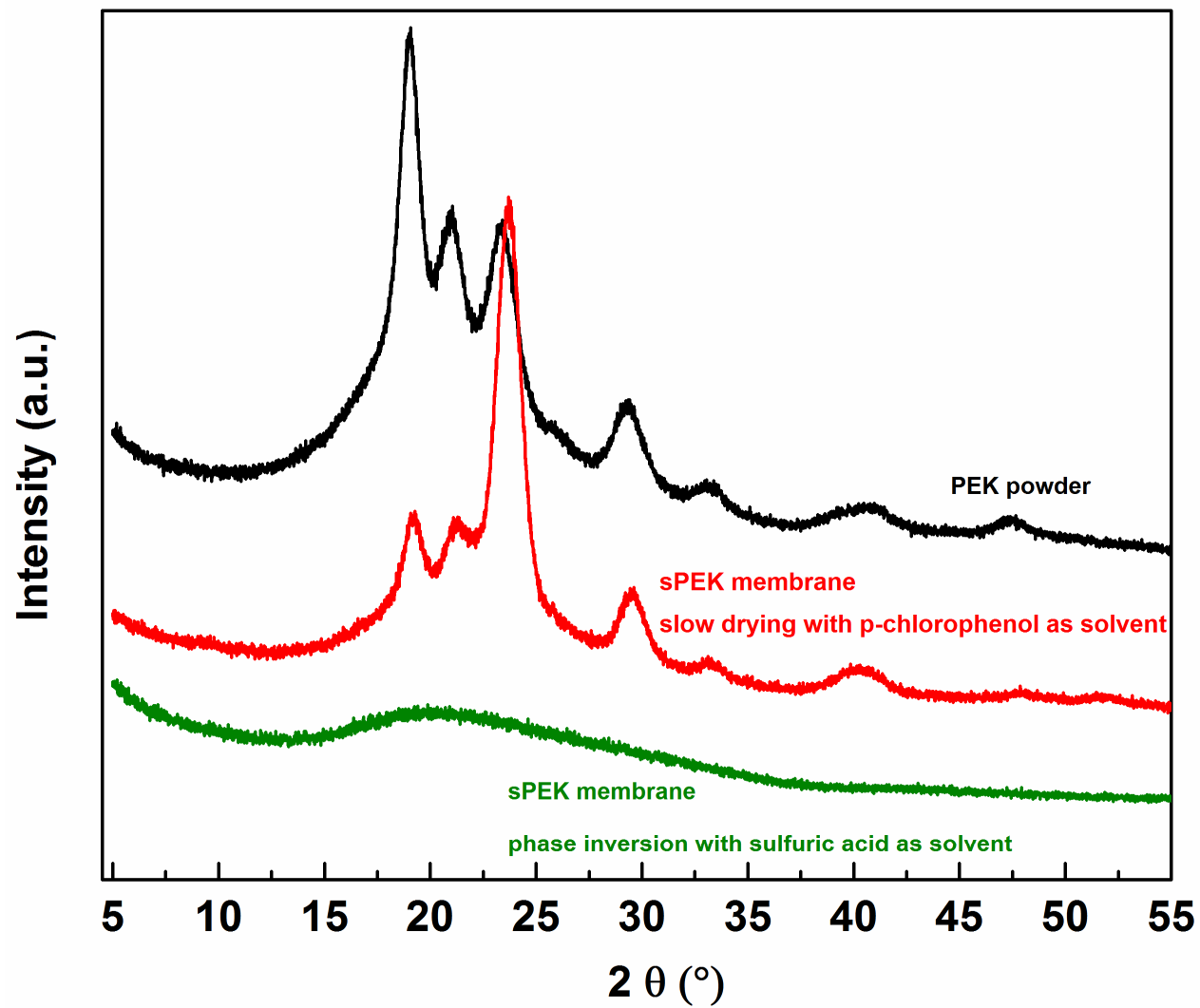


Figure S1 XRD patterns of PEK powder and sPEK membranes cast with different solvents.

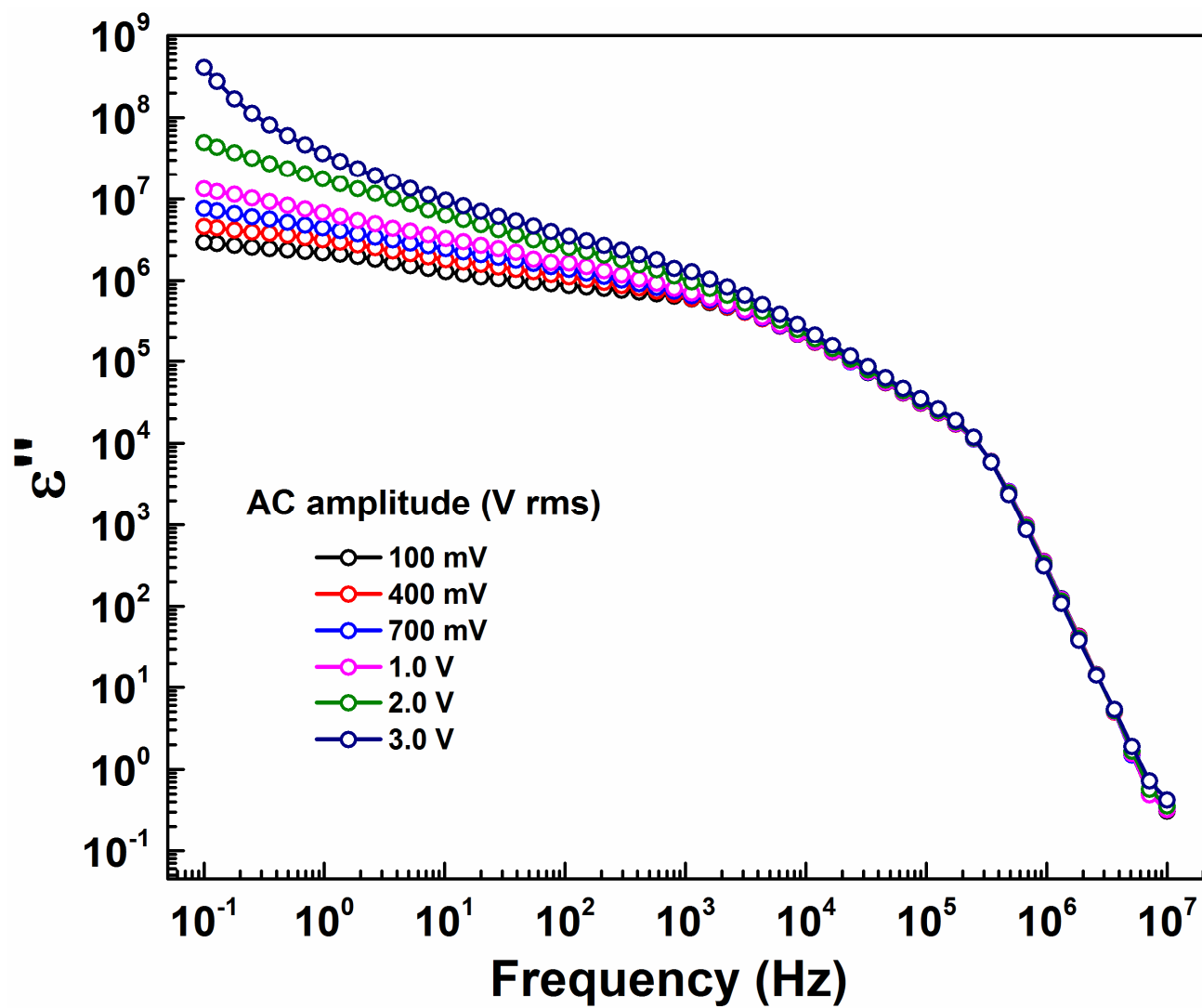
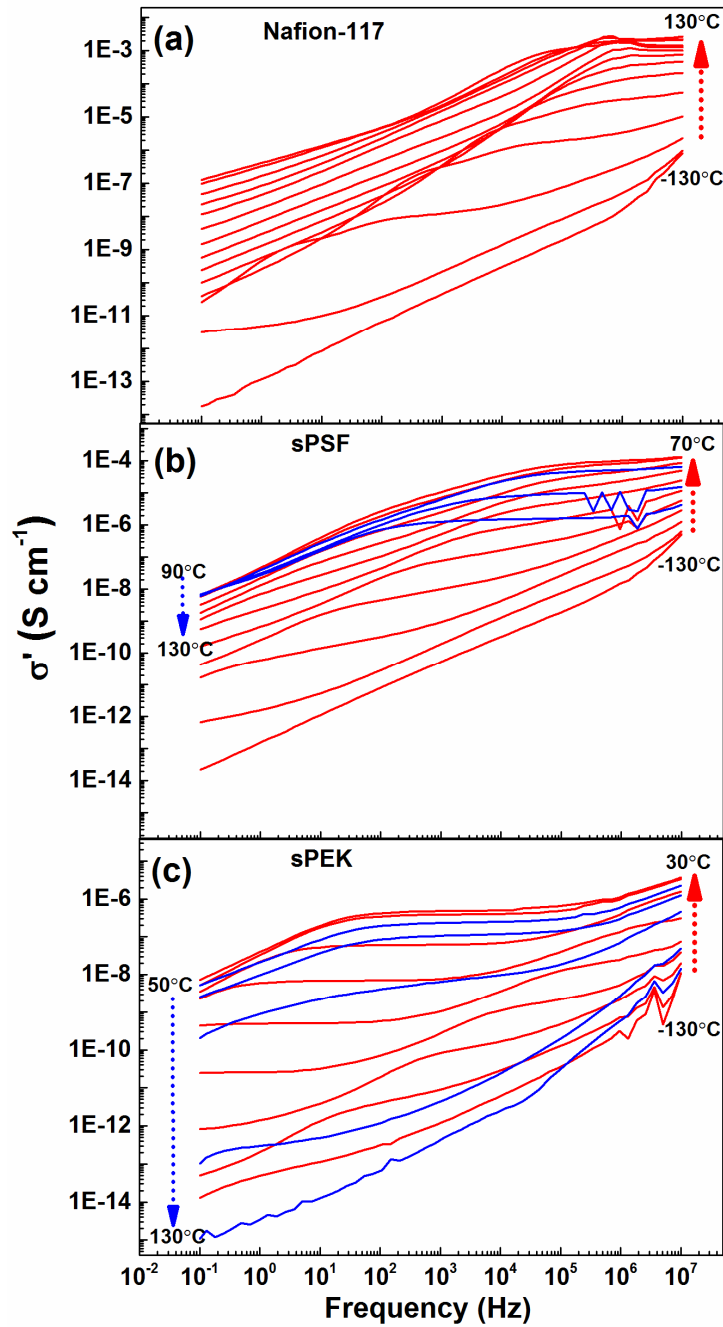
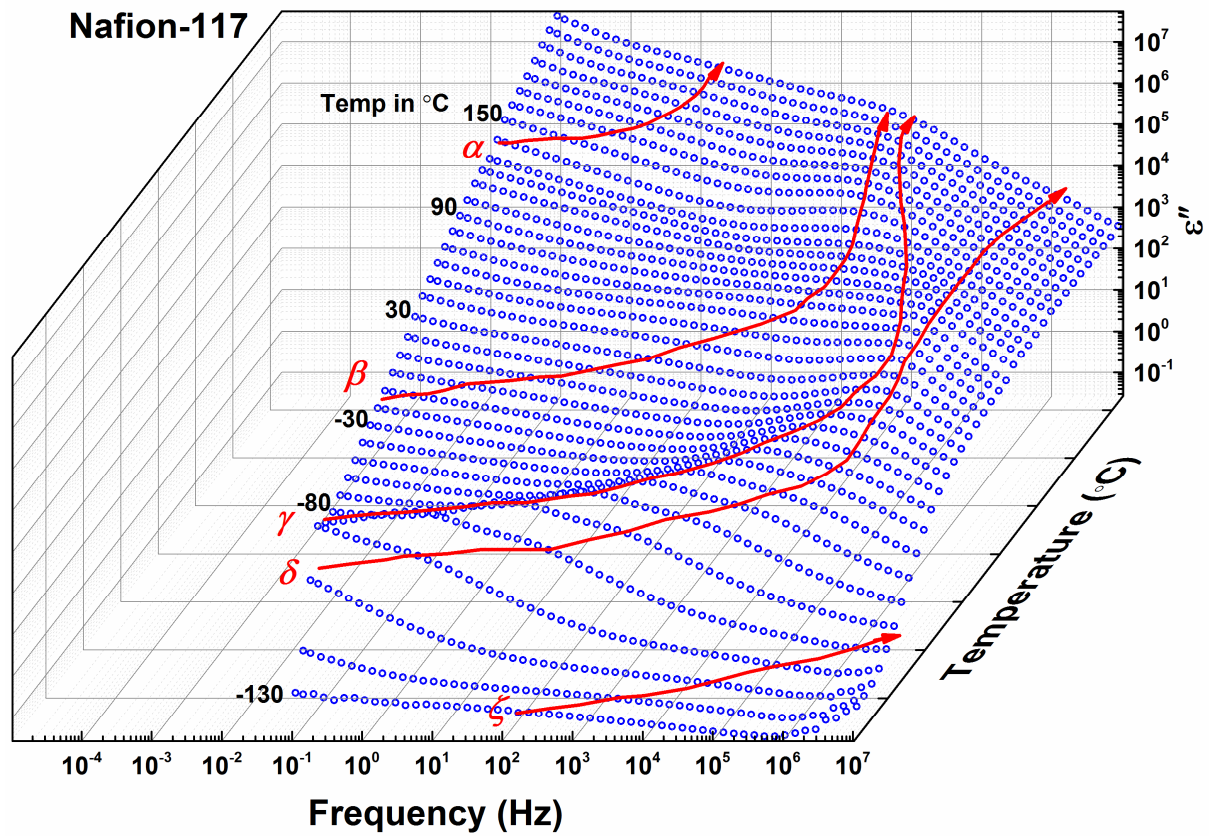


Figure S2 Dielectric loss ( $\epsilon''$ ) of Nafion-117 at various ac amplitudes.



**Figure S3** Proton conductivity calculated from the Nyquist plot at all the frequencies from BDS of Nafion-117 (a), sPSF (b), and sPEK (c) membranes in the temperature range of -130 – 130°C (every 20°C). The red lines indicate the increasing trend (upward arrow), while, the blue lines show the decreasing trend (downward arrow) in the conductivity.



**Figure S4** Waterfall plot of dielectric loss ( $\epsilon''$ ) as a function of frequency and temperature with Nafion-117 membrane.

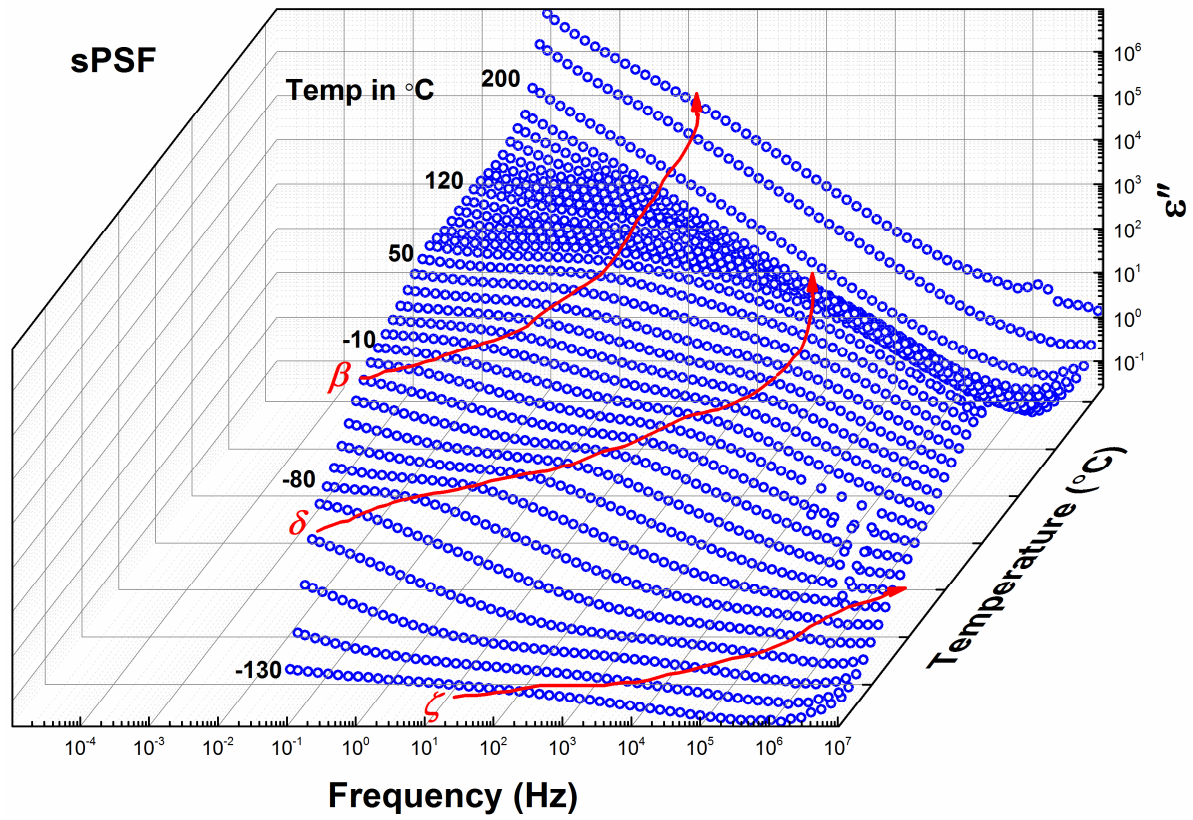


**Figure S5** Waterfall plot of dielectric loss ( $\epsilon''$ ) as a function of frequency and temperature with sPSF membrane.

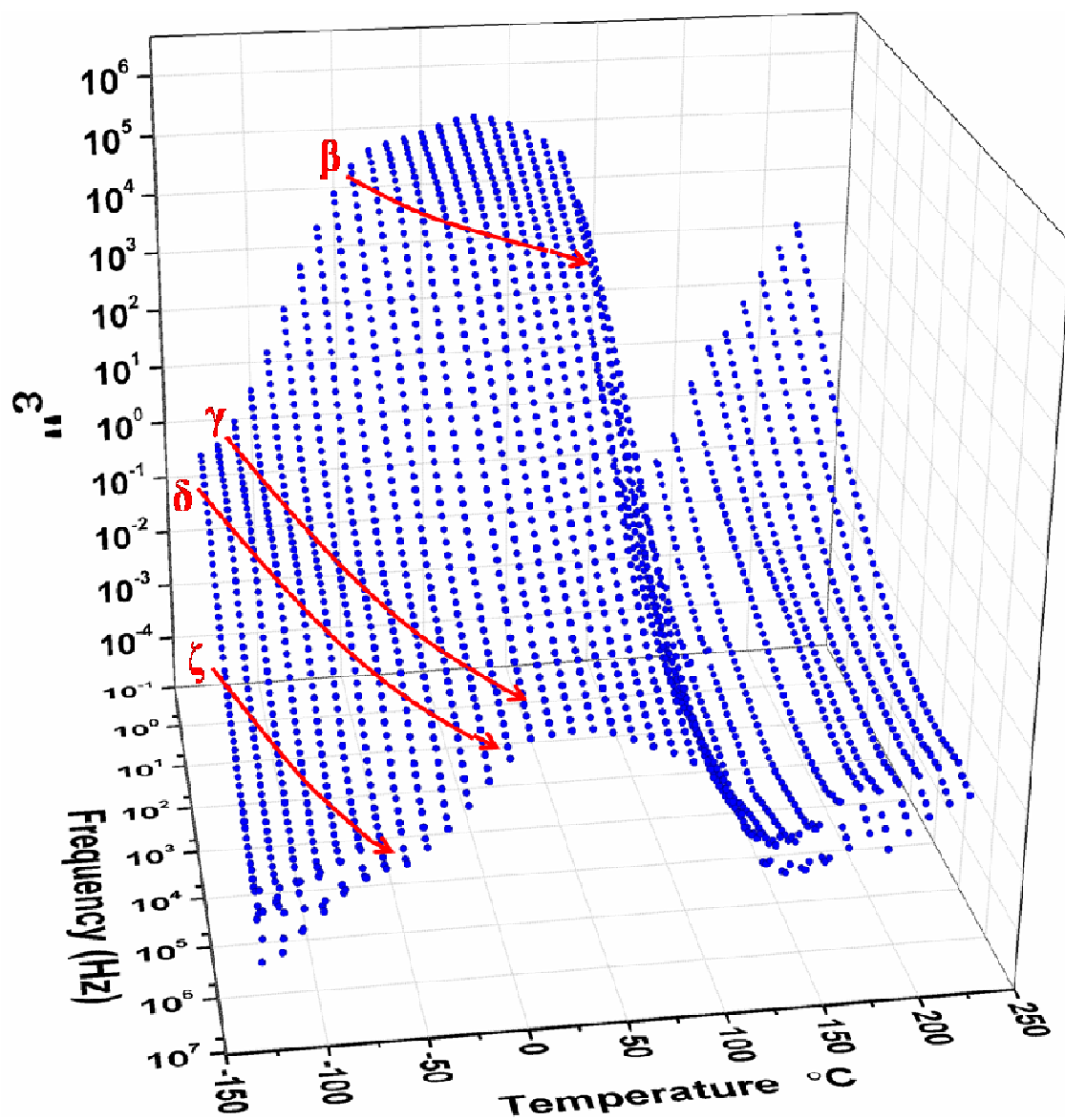
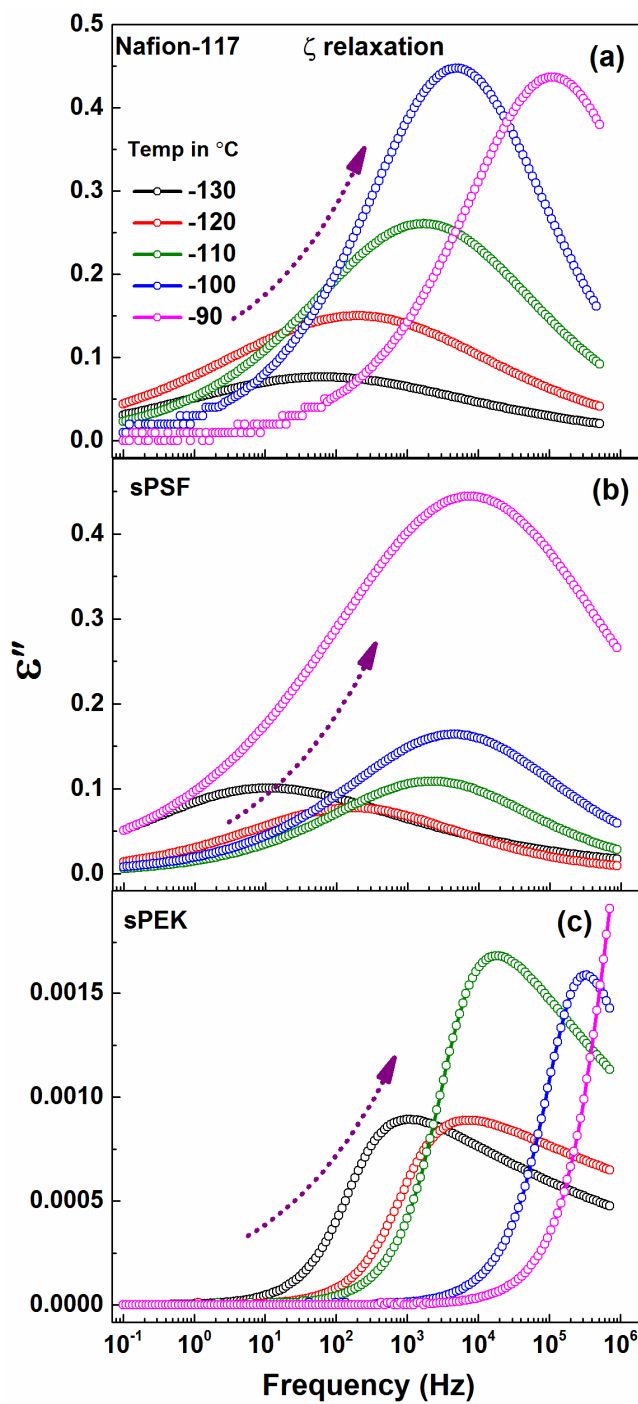
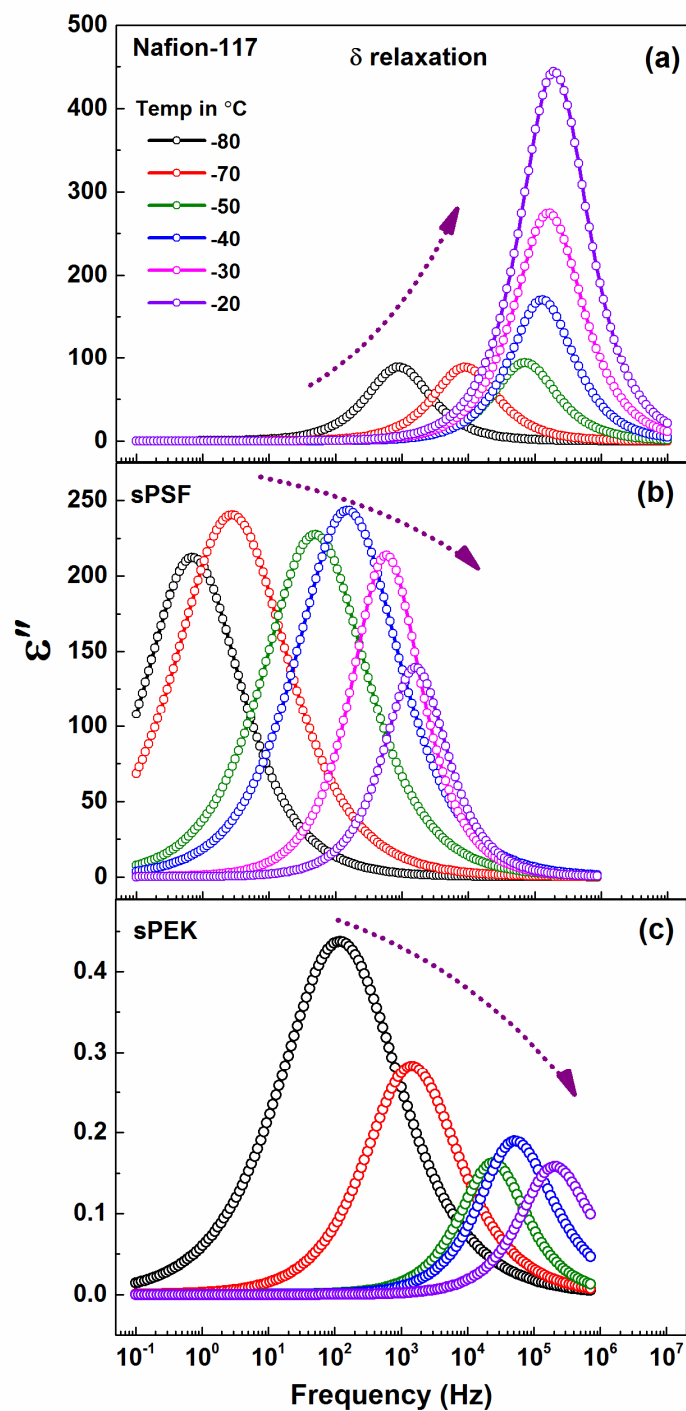


Figure S6 Dielectric loss ( $\epsilon''$ ) as a function of frequency and temperature with sPEK membrane.





**Figure S7** The  $\zeta$  relaxation peak with membranes of Nafion-117 (a), sPSF (b), and sPEK (c) in the temperature range of -130 – -90°C. The arrows indicate the movement of the relaxation peaks and the change in intensity of  $\epsilon''$ .



**Figure S8** The  $\delta$  relaxation ( $-\text{SO}_3\text{H}$ ) peak with membranes of Nafion-117 (a), sPSF (b) and sPEK (c) in the temperature range of  $-80 - -20^\circ\text{C}$ . The arrows indicate the movement of the relaxation peaks and the change in intensity of  $\epsilon''$ .

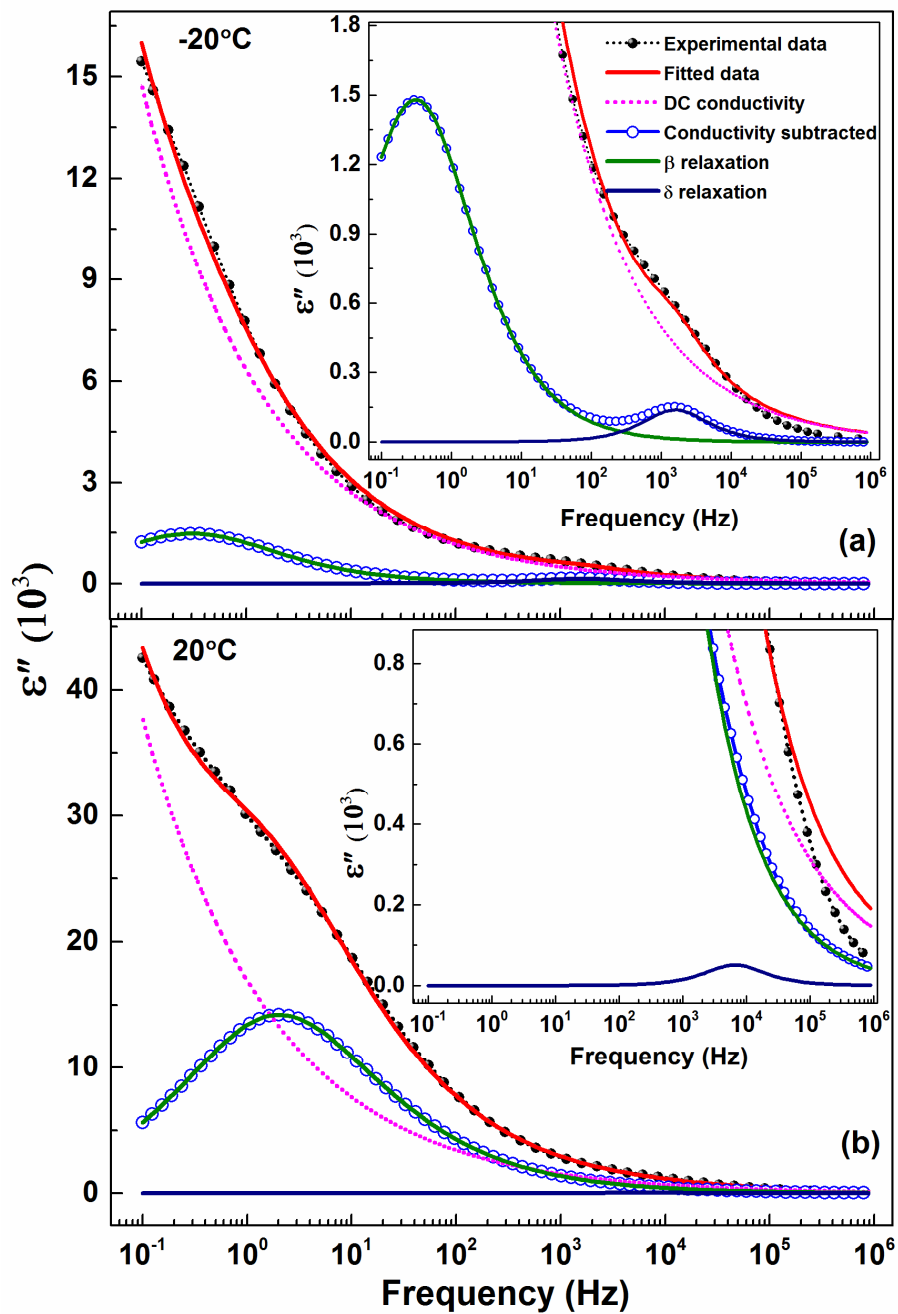


**Figure S9** Dielectric loss ( $\epsilon''$ ) data of sPSF membrane at a temperature of  $-20^\circ\text{C}$  (a) and  $20^\circ\text{C}$  (b) fitted with 2 HN functions.

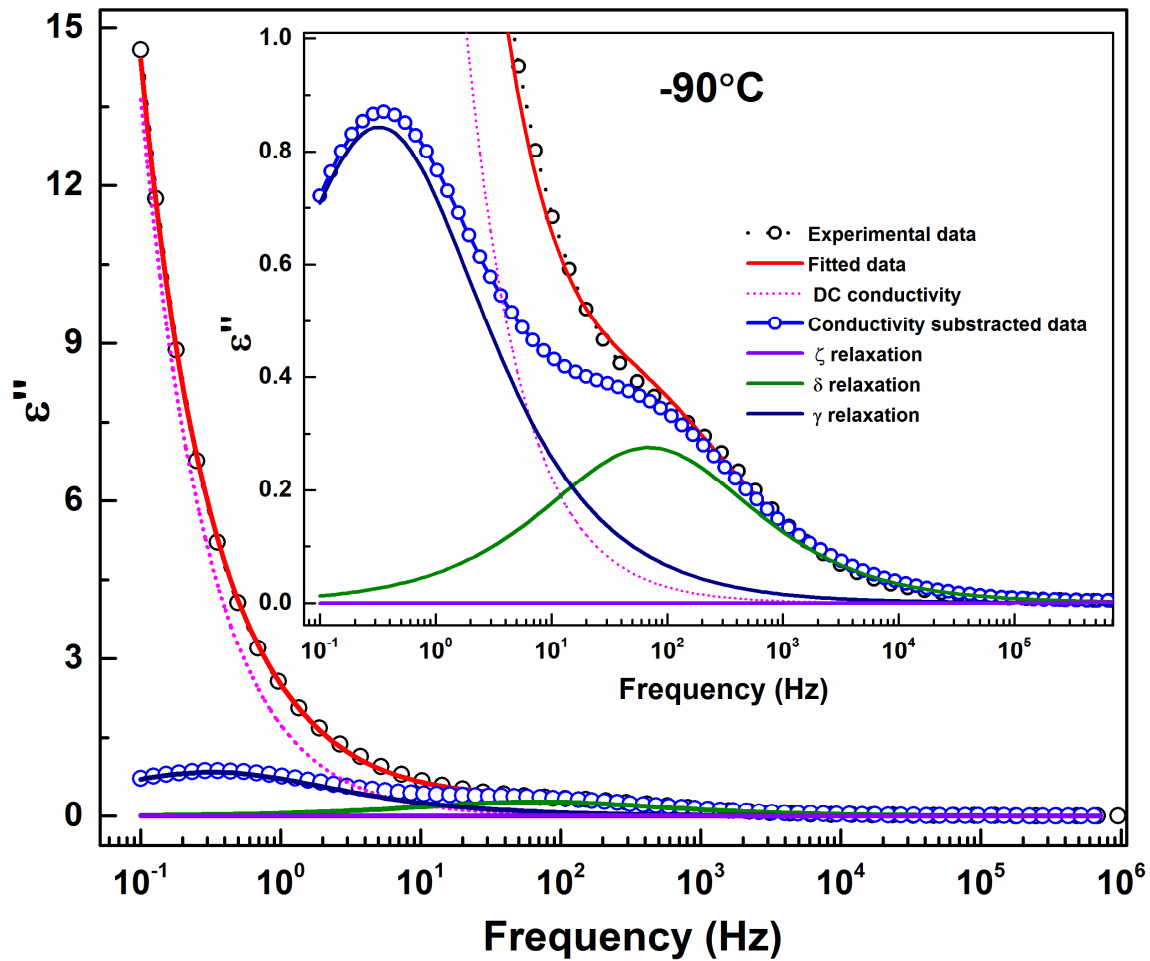


**Figure S10** Dielectric loss ( $\epsilon''$ ) data of SPEK membrane at a temperature of  $-90^\circ\text{C}$  fitted with 3 HN functions.

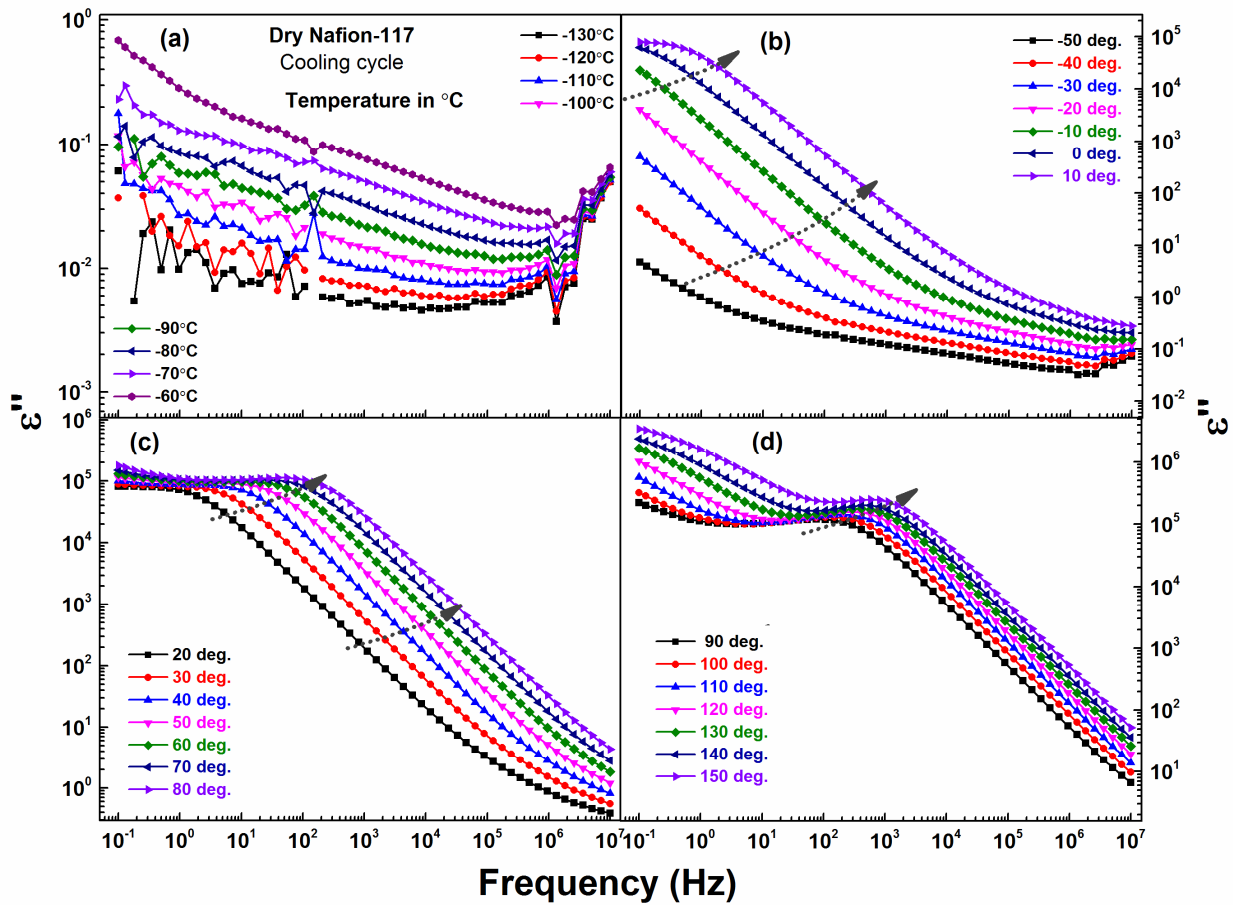


**Figure S11** Dielectric loss ( $\epsilon''$ ) as a function of frequency at various temperatures (cooling cycle) for dry Nafion-117 membrane.

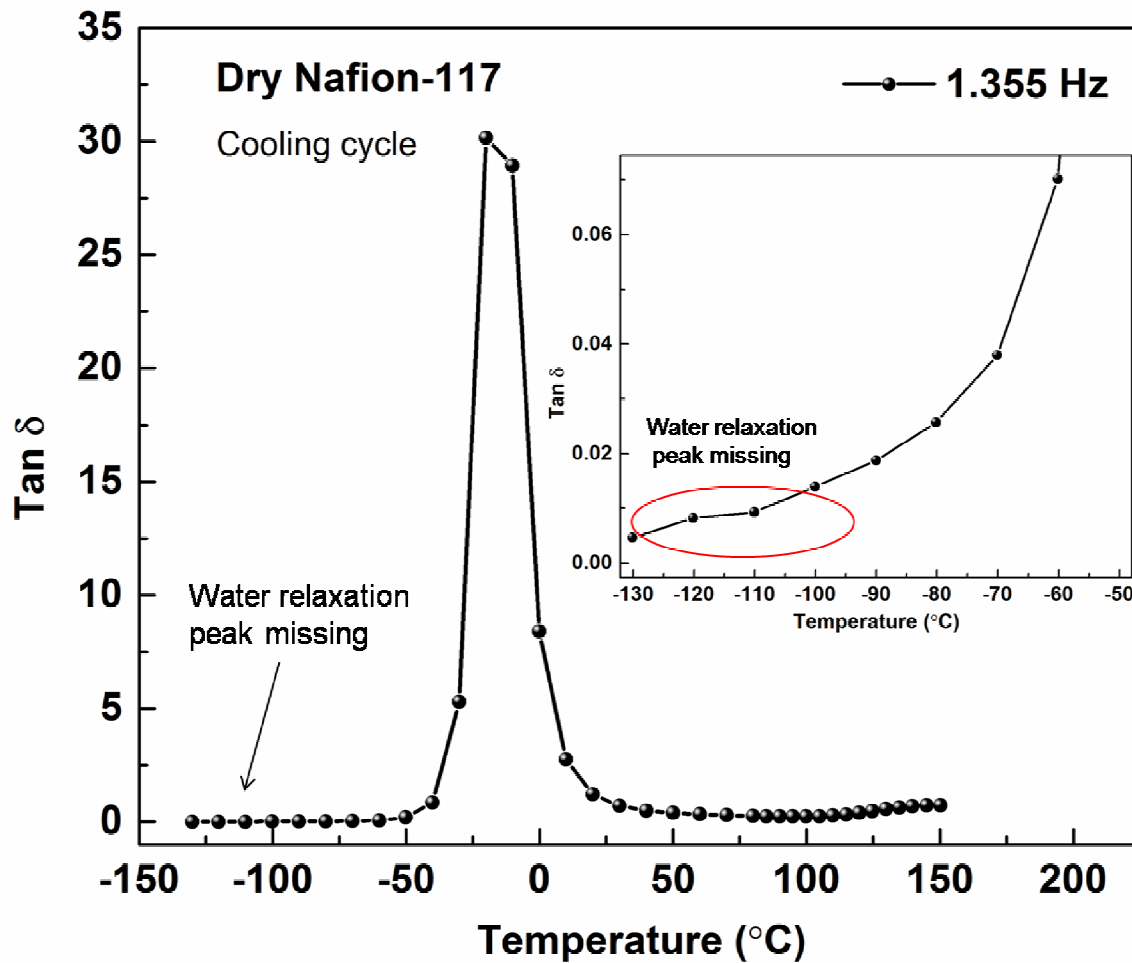


**Figure S12** Tan  $\delta$  at a frequency of 1.355 Hz as a function of temperature with dry Nafion-117; inset shows the magnified view of the spectrum at very low temperatures.

## Activation energy calculation

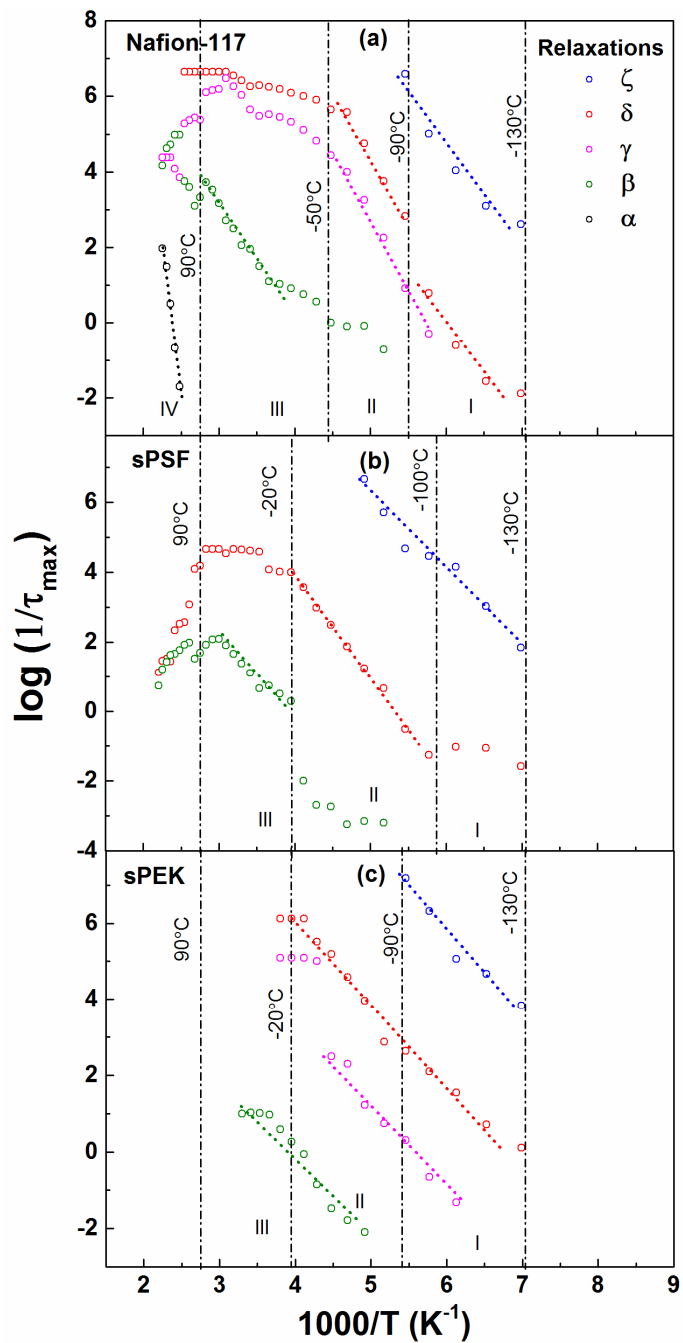


**Figure S13** Temperature dependence of the relaxation time with membranes of Nafion-117 (a), sPSF (b) and sPEK (c). Dotted lines indicate the change in slope and are divided into different zones (I, II, III and IV).

The activation energy of the various relaxations of all the three membranes is calculated from the  $\log (1/\tau_{\max})$  vs  $1000/T$  plot.<sup>1</sup>

$$\tau = \tau_0 \exp \left[ \frac{-E_A}{RT} \right] \dots\dots\dots(1)$$

where,  $\tau$  is the relaxation time,  $\tau_0 = 1/2\pi f$ ,  $E_A$  is the activation energy and  $R$  is the universal gas constant.

In general, the relaxations of all the three membranes show Arrhenius behavior. However, slight changes in the slopes can be observed; sPSF shows higher slope while Nafion has lower slope for  $\zeta$  relaxation. Depending on the transition of the relaxation process and the change in slope, the plot is divided to different zones (I, II, III and IV). The activation energy corresponding to each of the relaxation of all the three membranes is shown in **Table S1**.

**Table S1.** Activation energies of various relaxations of Nafion-117, sPSF and sPEK membranes.

Membrane	Region	Activation energy (kJ mol <sup>-1</sup> )				
		Relaxations				
		$\zeta$	$\delta$	$\gamma$	$\beta$	$\alpha$
Nafion-117	I	38.10	59.35	-	-	-
	II	-	58.97	72.18	-	-
	III	-	-	-	60.48	-
	IV	-	-	-	-	326.45
sPSF	I	40.4	-	-	-	-
	II	-	51.33	-	-	-
	III	-	-	-	51.12	-
sPEK	I	41.35	44.62	-	-	-
	II	-	-	41.26	49.78	-



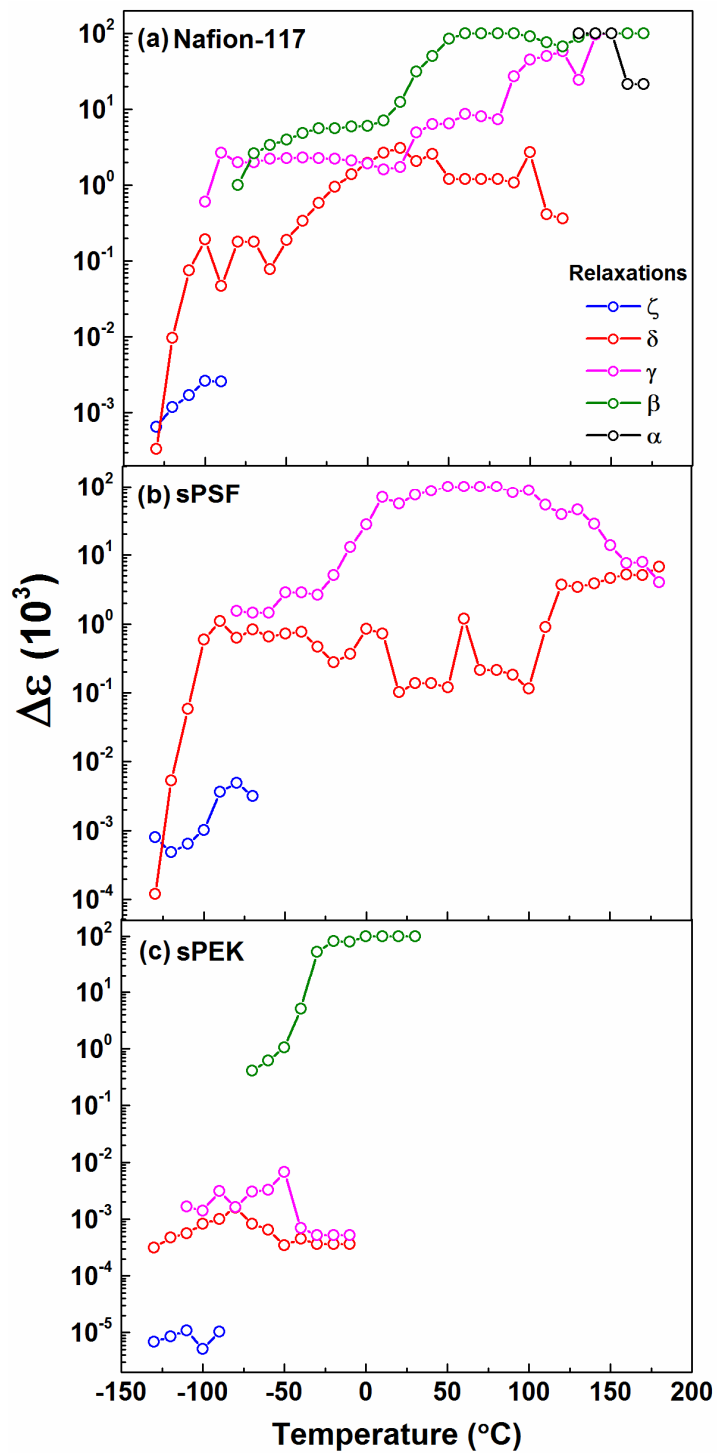


**Figure S14** Dielectric strength ( $\Delta\epsilon$ ) of the different relaxations with membranes of Nafion-117 (a), sPSF (b), and sPEK (c).

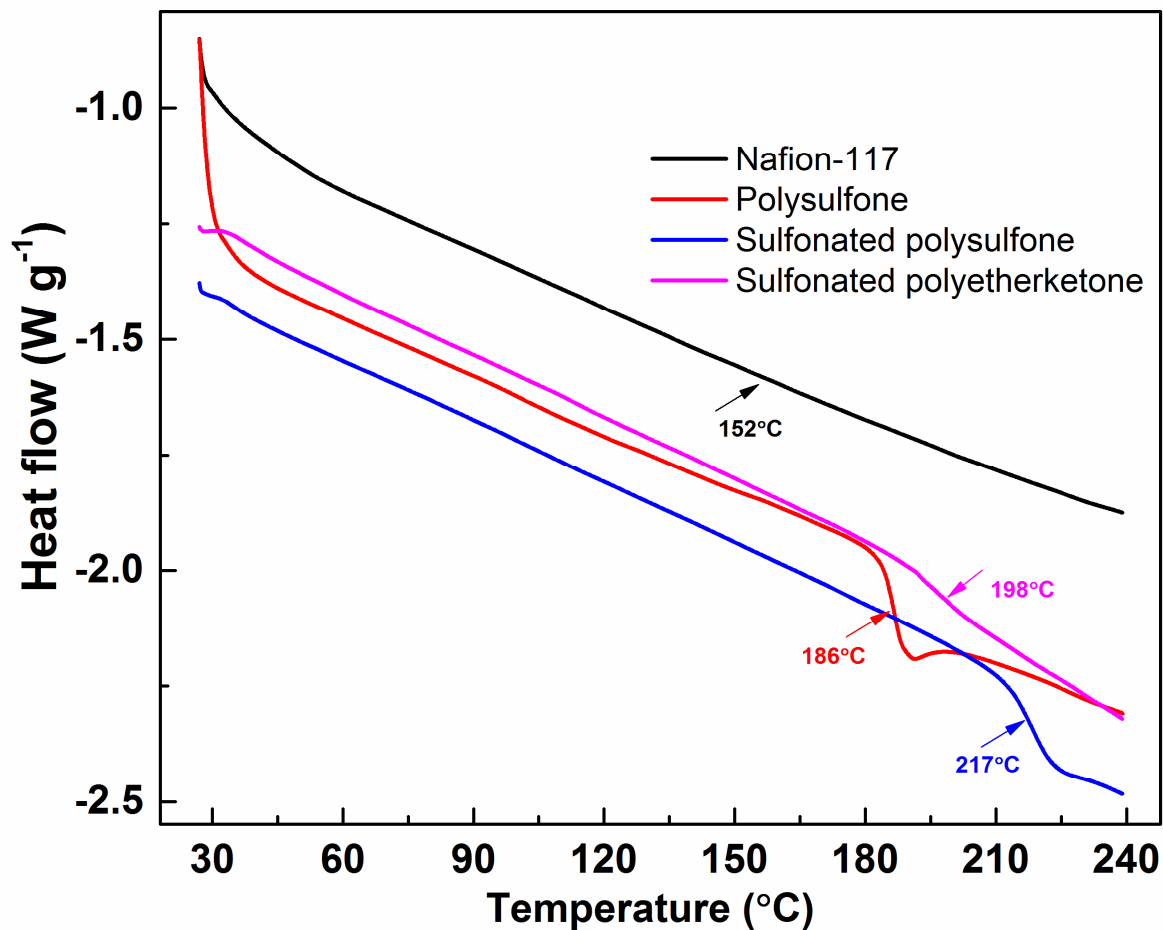


**Figure S15** DSC thermograms of Nafion-117, PSF, sPSF and sPEK membranes; the second heating cycle was used to calculate the  $T_g$ .

## REFERENCES

1. Kremer, F., Tsuwi, J., Pospiech, D., Jehnichen, D. and Ha, L. *J. Appl. Polym. Sci.* **2007**, *105*, 201–207.

